LEVEL II

(12)

RADC-TR-80-191
Final Technical Report
June 1980

A080566

COLUMN NETWORK STUDY FOR A PLANAR ARRAY USED WITH AN UNATTENDED RADAR

Sperry Gyroscope Company

Gerald L. Hanley
Harry R. Perini

ROME AIR DEVELOPMENT CENTER
Air Force Systems Command
Griffiss Air Force Base, New York 13441

This report has been reviewed by the RADC Public Affairs Office (PA) and is releasable to the National Technical Information Service (NTIS). At NTIS it will be releasable to the general public, including foreign nations.

RADC-TR-80-191 has been reviewed and is approved for publication.

APPROVED: Gregory Cruz

GREGORY CRUZ, 1Lt, USAF
Project Engineer

APPROVED: Allan C. Schell

ALLAN C. SCHELL, Chief
Electromagnetic Sciences Division

FOR THE COMMANDER: John P. Huss

JOHN P. HUSS
Acting Chief, Plans Office

SUBJECT TO EXPORT CONTROL LAWS

This document contains information for manufacturing or using munitions of war. Export of the information contained herein, or release to foreign nationals within the United States, without first obtaining an export license, is a violation of the International Traffic in Arms Regulations. Such violation is subject to a penalty of up to 2 years imprisonment and a fine of $100,000 under 22 U.S.C 2778.

Include this notice with any reproduced portion of this document.

If your address has changed or if you wish to be removed from the RADC mailing list, or if the addressee is no longer employed by your organization, please notify RADC (EEA) Hanscom AFB MA 01731. This will assist us in maintaining a current mailing list.

Do not return this copy. Retain or destroy.

UNCLASSIFIED

SECURITY CLASSIFICATION OF THIS PAGE (When Data Entered)

(19) REPORT DOCUMENTATION PAGE		READ INSTRUCTIONS BEFORE COMPLETING FORM
(1) 1. REPORT NUMBER RADC-TR-80-191	2. GOVT ACCESSION NO. AD-A087 809	3. RECIPIENT'S CATALOG NUMBER
(6) 4. TITLE (and Subtitle) COLUMN NETWORK STUDY FOR A PLANAR ARRAY USED WITH AN UNATTENDED RADAR		5. TYPE OF REPORT & PERIOD COVERED Final Technical Report Dec 78 - Feb 80
	(14)	6. PERFORMING ORG. REPORT NUMBER SG-4253-1182
(10) 7. AUTHOR(s) Gerald L. Hanley Harry R. Perini (12) 65	(15)	8. CONTRACT OR GRANT NUMBER(s) F19628-78-C-0166
9. PERFORMING ORGANIZATION NAME AND ADDRESS Sperry Gyroscope Company Great Neck LI 11020	(16)	10. PROGRAM ELEMENT, PROJECT, TASK AREA & WORK UNIT NUMBERS 12412F 24480119 (17) 02
11. CONTROLLING OFFICE NAME AND ADDRESS Deputy for Electronic Technology (RADC/EEA) Hanscom AFB MA 01731	(11)	12. REPORT DATE June 1980 13. NUMBER OF PAGES 68
14. MONITORING AGENCY NAME & ADDRESS(if different from Controlling Office) Same (9) Final Technical rept. Dec 78-Feb 80's		15. SECURITY CLASS. (of this report) UNCLASSIFIED
		15a. DECLASSIFICATION/DOWNGRADING SCHEDULE N/A

16. DISTRIBUTION STATEMENT (of this Report)

Approved for public release; distribution unlimited.

17. DISTRIBUTION STATEMENT (of the abstract entered in Block 20, if different from Report)

Same

18. SUPPLEMENTARY NOTES

RADC Project Engineer: Gregory Cruz, 1Lt (RADC/EEA)

19. KEY WORDS (Continue on reverse side if necessary and identify by block number)

Column Network
Planar Array
Stripline
Dual Beam

20. ABSTRACT (Continue on reverse side if necessary and identify by block number)

Objectives of this program are to investigate design and fabrication techniques for an azimuthally phase-steerable planar array with dual beams for elevation coverage. Network costs, network insertion loss, antenna pattern performance, and reliability are significant considerations. A stripline dual beam column network is being designed, fabricated and tested to demonstrate achievable performance and competitive techniques for production and installation costs are being studied. (Cont'd)

DD FORM 1 JAN 73 1473 EDITION OF 1 NOV 65 IS OBSOLETE

UNCLASSIFIED

SECURITY CLASSIFICATION OF THIS PAGE (When Data Entered)

330800

Item 20 (Cont'd)

This report summarizes the work completed during the program: completion of the antenna conceptual design, development of all the required components, design of the dual beam column network, and results of competitive techniques for production.

EVALUATION

1. This is a Final Report on the contract covering the period December 1978 to February 1980. The objective of this program was to investigate, design and fabricate techniques for a column network for an azimuthally phase-steerable planar array with dual beams for elevation coverage. Consideration was given to network costs, network insertion loss, antenna pattern performance and reliability. This effort was directed toward reducing operating costs associated with the present DEW line system, as well as to improve present surveillance coverage against low flying targets.

2. In the period available a stripline dual beam column network was designed, fabricated with the use of Computer-Aided-Design equipment and tested to substantiate the design objectives. An overall antenna system configuration study was performed to examine the baseline antenna design. Also an investigation of fabrication techniques for the stripline column network was performed with emphasis on electrical performance, cost, structural integrity and lightweight.

3. The findings detailed in the report are proving of great value to the effort within RADC/EEA in the development of phased array technology.

GREGORY CRUZ, 1Lt, USAF
Project Engineer

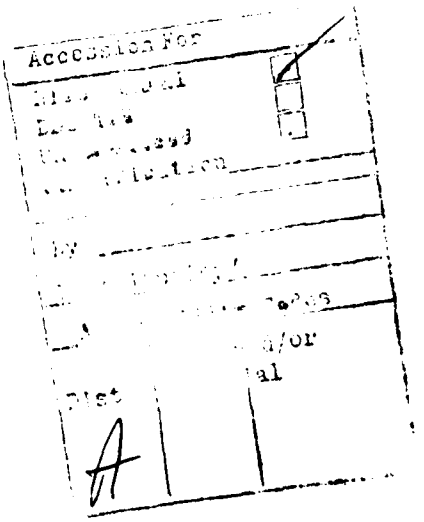

CONTENTS

LIST OF ILLUSTRATIONS

TABLES

Section 1

INTRODUCTION

The objectives of this program were to investigate design and fabrication techniques for an azimuthally phase-steerable planar array with dual beams for elevation coverage. The potential application is for unattended strategic ground radar systems which will be located in remote arctic areas. The unattended radars are intended to be a means of reducing operating costs associated with the present DEW Line system, as well as to improve present surveillance coverage against low flying targets. Network costs, network insertion loss, antenna pattern performance, and reliability are significant considerations.

A stripline dual beam column network which was designed, fabricated and tested as part of this program, demonstrated compliance with the aforementioned objective. Analysis of fabrication techniques showed a pressed-laminate assembly technique will yield a production cost of $300 and a weight of 9 pounds for a 12 foot, L-band dual channel network. The networks were designed and developed to supply an amplitude and phase aperture illumination for a specified dual beam pattern performance. Theoretical and experimental studies were performed on propagation characteristics of inhomogeneously filled strip transmission lines. This effort was followed by a componenet development effort for couplers, crossover networks, dipole radiators, and low cost terminators. The network design was simplified by the use of Computer-Aided-Design equipment for the generation of artwork and photo-masks for the fabrication of large stripline networks. A dual-beam network was then fabricated which generated a pencil beam which covered from 0 to 5 degrees and a $\csc^2$ beam shape from 5 to 30 degrees. The experimental results obtained substantiated the design procedures used. The beam shape, sidelobe performance, insertion loss, and VSWR meets the design objectives.

Section 2 is an overall antenna system configuration study to examine the baseline antenna design, to evaluate antenna performance, and to study component packaging, assembly concepts, structural requirements and environmental factors.

Section 3 describes the design and fabrication of a large stripline dual beam column network for use in the baseline antenna design. A photo of the completed network and measured electrical performance are presented in this section.

Section 4 describes the investigation of fabrication techniques for the stripline column network with emphasis on electrical performance, ease of manufacturing, cost, structural integrity and lightweight.

Section 5 describes the development program for the individual microwave components used in the design of the stripline dual beam column network.

Section 2

ANTENNA CONFIGURATION STUDIES

2.1 TASK SUMMARY

This section describes an investigation of the design and fabrication techniques for a 2-D, azimuthally steerable, four-faced planar array for application to unattended, ground-based, search radars. The design approach utilizes a square configuration of four planar phased arrays to provide 360-degree azimuthal surveillance coverage to fifteen thousand feet in altitude, with an instrumented range of sixty nautical miles. The elevation coverage is achieved using two contiguous beams which provide coarse target elevation data and facilitate the use of optimized signal processing techniques for low and high elevation targets independently. To achieve this elevation coverage, the four planar arrays contain vertical column networks comprising radiator elements and low loss microwave power distribution networks. The network is capable of simultaneously generating the illumination function for the low and high beams, respectively, through discrete input ports. An objective of this task effort is to identify the requirements imposed upon the column network by selection of the baseline antenna design.

The workscope associated with this task involves (1) examination of the baseline antenna design, (2) antenna performance evaluation, (3) definition of physical parameters, component packaging, and assembly concept, (4) evaluation of structural requirements and environmental impact factors, and (5) conceptual design selection. The study results are described in the following subsections.

2.2 BASELINE ANTENNA DESCRIPTION

A baseline antenna configuration has been generated consisting of four planar array faces mounted in a square configuration on top of a tower platform. Each array provides coverage against airborne targets at elevations from ground level to fifteen thousand feet and within an instrumented range of sixty nautical miles. Dual fixed beam elevation coverage permits separate, independent, signal processing techniques for the two elevation regimes. Phase steerable azimuth scan capability provides $\pm$ 45-degree coverage from each array face, thereby enabling a full 360-degree azimuth coverage. The antenna is designed for installation and operation in a severe arctic environment as part of an unattended radar system. As such, its components are designed for low loss, high reliability, low power consumption, and easy maintainability.

The baseline antenna configuration, figure 2-1, consists of four 12 by 24-foot planar arrays mounted in a square configuration on a tower with a maximum height of 100 feet. Each array face consists of 59 vertical column network boards spaced 4.9 inches apart. The tower structure will have its legs sunk into an excavation deep enough to stand on perpetually frozen ground. The array and mounting structure are designed to withstand the extremes of arctic operation, including wind velocities of 100 mph, ambient temperatures varying between -35 and +100 degrees Fahrenheit, and peak snow loading.

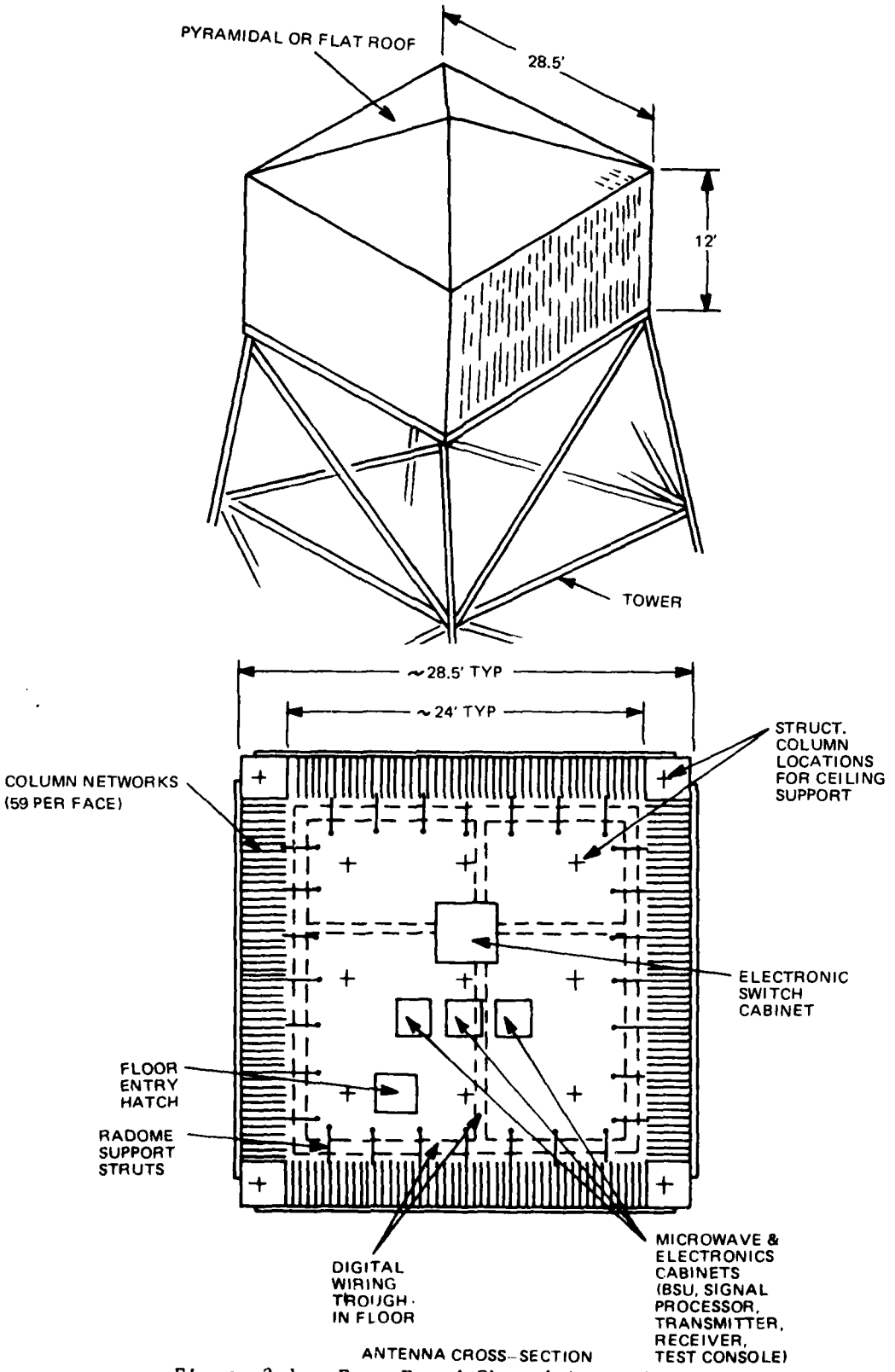

Figure 2-1. Four-Faced Phased Array Antenna

The basic antenna structure is envisioned as a one-piece, floor and ceiling structure, with a modularized radome consisting of fiberglass sandwich panels, each being 5 feet wide by 12 feet high. The floor structure interfaces with the tower deck and contains false flooring for electrical cables, mounting provisions for the electronic cabinets, and personnel entry hatches. The floor structure is designed to transmit all vertical and horizontal loads and moments, due to equipment weight, snow, ice, and wind loads, directly to the tower structure. The ceiling structure is sized to withstand the design snow loads for the arctic application. These loads are transmitted to the floor structure by means of vertical structural columns tying the two structures together. The columns effectively unload the radome panels with respect to vertical loads caused by snow and ceiling dead weight, resulting in a radome which is sized to withstand only the design wind and icing loads. Both the floor and ceiling structures are thermally insulated, and contain mounting provisions for the radome by means of flanges around the periphery. These structures also contain slide mechanisms to position the 12-foot high column networks which are inserted from the interior, toward the radome surface.

The multi-sectioned radome design affords ease of fabrication, reduced manufacturing costs, and eased transportability requirements over a one-piece planar design. The individual radome panels are supported at their lower and upper ends by the floor and ceiling, respectively, and are butted together to create a site-erected, continuous surface. At the butted joint, the radome panels are bolted to a T-section column which lends vertical support. This column is further reinforced by a fiberglass block forward of the network dipoles. To limit allowable deflections under wind loading and radome panel stress levels, the vertical radome columns are supported at midspan by a pinned triangular frame structure, tied directly to the floor and ceiling structures.

A sketch of the radome joint design and the ground plane attachment for the column networks, is shown in figure 2-2. Figure 2-3 is a schematic representation of an array face, showing the radome, column network, row networks, phase shifters and cabling.

The antenna is designed to minimize complexity and on-site installation, while still maintaining a high degree of reliability. The vertical column networks would be assembled off-site in groups of approximately 10, forming six array panel subassemblies per array face. Prealignment and registration techniques would then be employed to facilitate on-site assembly, without the need for sophisticated and costly alignment procedures. Environmental protection for each array face is provided via a coated fiberglass radome cover sheet. Each of the column network boards are sealed at their ends by means of metal closures fastened to the ground planes. Structural rigidity and support are provided by the printed circuit board ground planes of the column networks. To obtain a high degree of reliability, cable interconnections are minimized.

Each vertical column network board will contain 25 printed dipole radiator elements and the associated stripline elevation feed circuitry. The baseline column network is 12 feet long, with a maximum depth of 27 inches at the center and a minimum depth of 15 inches at the board edges. Each board is estimated to weigh approximately 13 pounds, resulting in a total weight of about 800 pounds per array face.

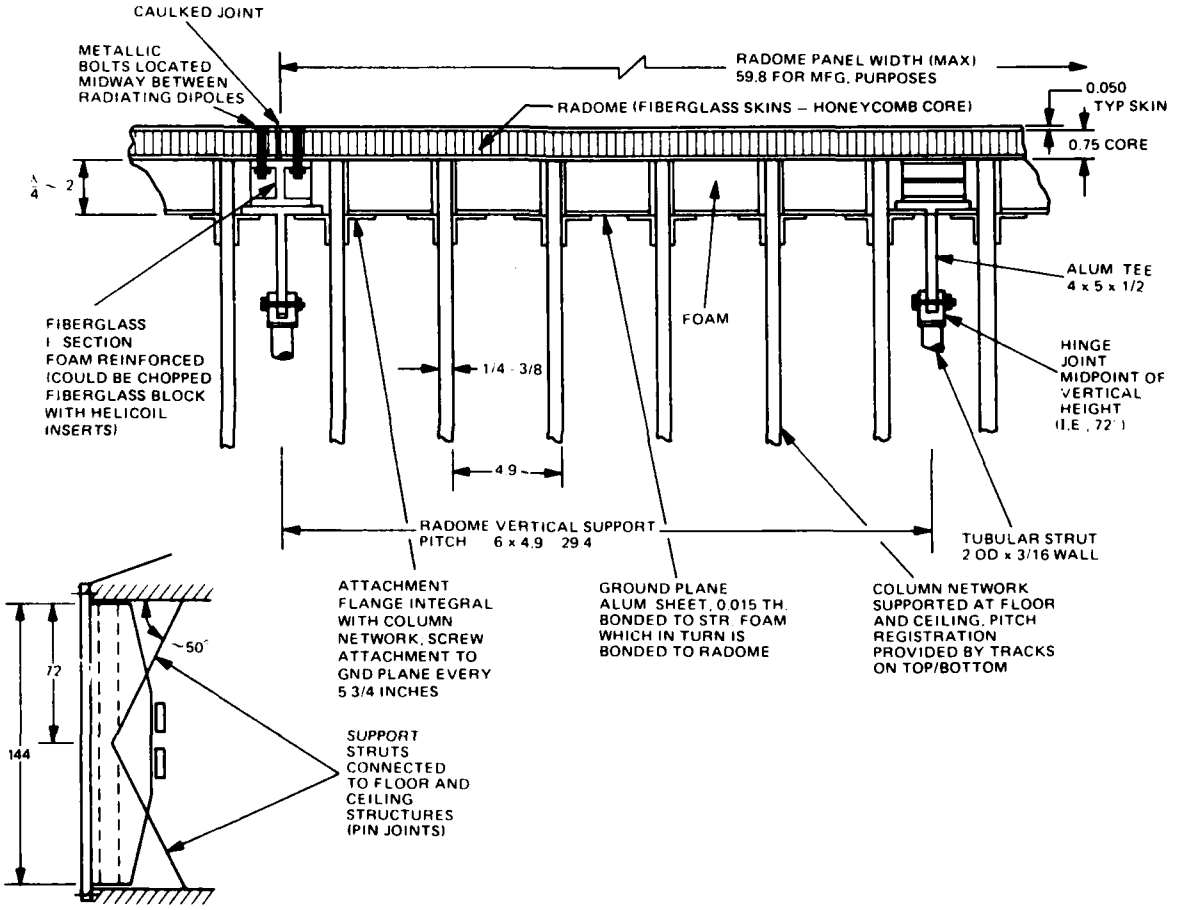

Figure 2-2. Structural Details of Ground Plane Connection and Radome Support Structures

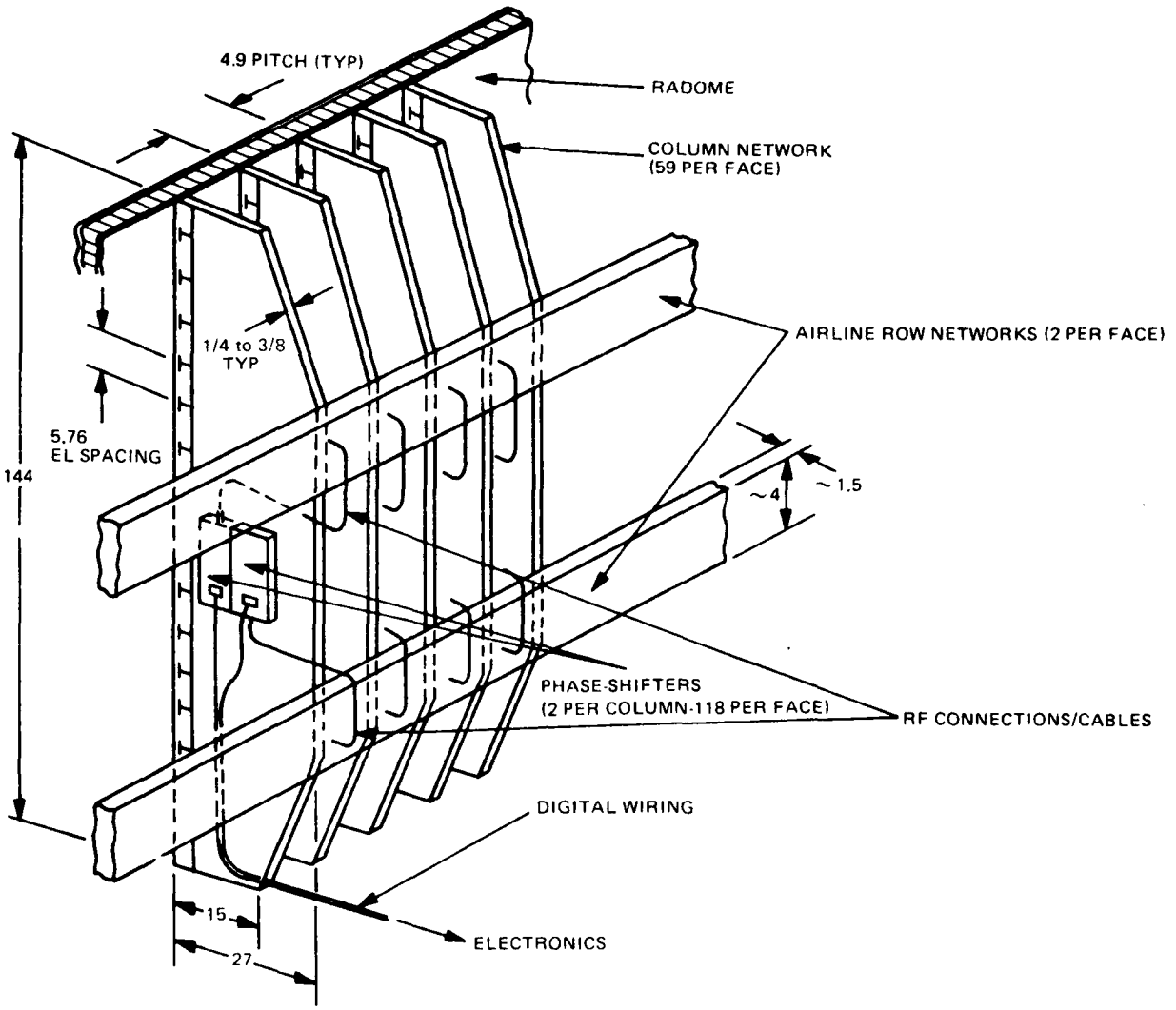

Figure 2-3. Schematic Representation of Array Face

2.3 FUNCTIONAL DESCRIPTION

The baseline antenna is designed to provide vertical polarization with constant gain coverage against airborne targets at elevations from ground level to five degrees above the horizon, and constant elevation coverage from five to thirty degrees above the horizon. To accomplish this, the antenna provides two simultaneous elevation beams generated via center-fed, dual-channel vertical column networks. The lower beam provides the constant gain coverage from 0 to 5 degrees; the upper beam provides a cosecant squared (constant elevation) coverage from 5 to 30 degrees. The antenna is phase steerable $\pm$ 45 degrees in azimuth via two separate sets of phase shifters.

Thus, simultaneous and independent control for each beam is realized, thereby enabling optimized processing algorithms to be utilized in each of the two channels.

A functional block diagram of the baseline antenna showing the key components, is presented in figures 2-4 and 2-5. Because of the quantities required, the vertical column network is a major key component. This is a low loss, single layer stripline, center-fed tandem series network which generates two independent array excitations corresponding to the two elevation beams. The stripline distribution network, designed to have less than 1.0 dB loss over the operating band, excites a set of printed stripline dipoles which are the vertically polarized radiating elements of the array.

The antenna is sized to provide a 2.0-degree azimuth beamwidth at the horizon. The elements are spaced for $\pm$ 45-degree azimuth scan for both beams, without any deleterious effect due to grating lobe conditions. Azimuth scan capability is provided via two sets of digital diode phase shifters. Diode phase shifters are used for the baseline antenna because of their inherent cost and packaging advantages at these frequencies. The required number of phase shifter bits is a function of the desired sidelobe performance. For the 25-dB baseline sidelobe design, 5-bit phase shifters are selected.

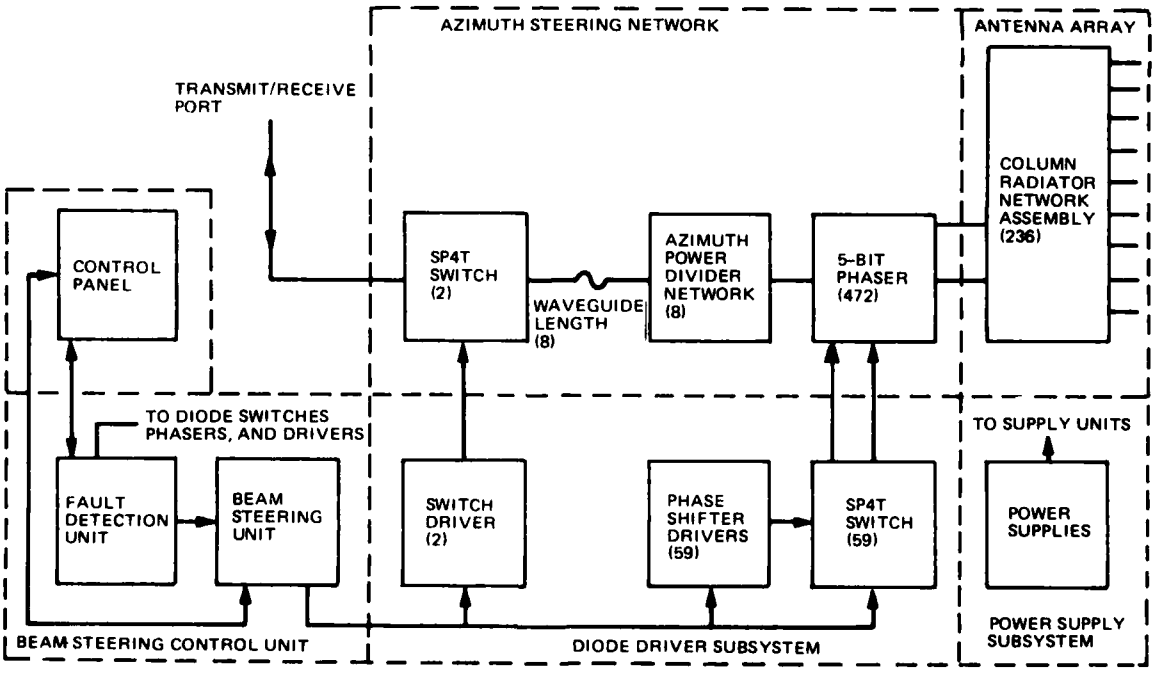

Figure 2-4. Four-Faced Planar Array, Block Diagram

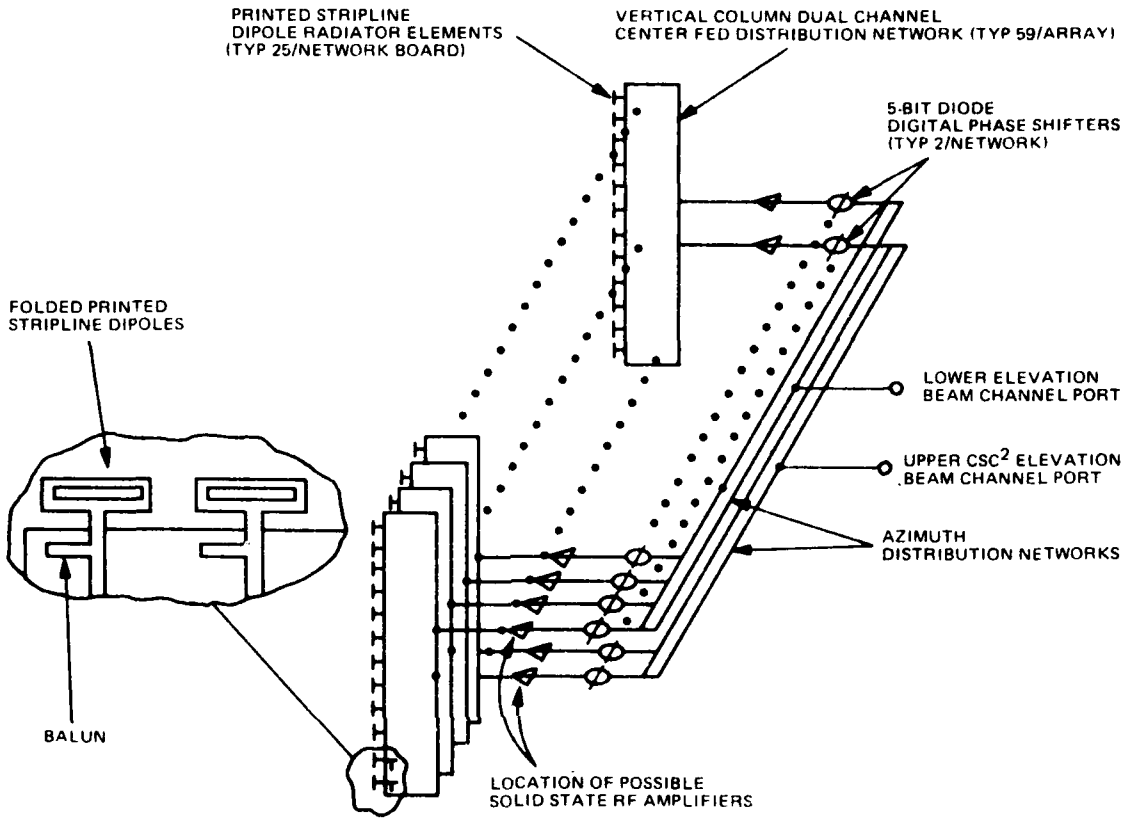

Figure 2-5. Antenna, Functional Diagram

To satisfy the dual shaped beam requirments, while still maintaining minimum loss in the feed network, each beam excitation is selected from a set of orthogonal beams employing complex weights. This approach provides selection of optimum beam shapes, while use of the center-fed tandem series column network enables independent generation of each beam excitation with a maximum degree of flexibility, minimum network loss, and better than -20 dB isolation between beam channels.

2.4 ARRAY ANTENNA PERFORMANCE

The performance objectives for the baseline antenna are consistent with the selected four-faced planar array configuration. Table 2-1 summarizes the key physical features and performance parameters for the baseline antenna concept.

Table 2-1. Baseline Antenna Summary Description

Antenna Type	Square four-faced Planar phased array
Frequency Band	1.2 to 1.4 GHz
Azimuth Coverage	360°
Elevation Coverage	0 to 15,000 feet
Design Features	Low loss, high reliability and easy maintainability for severe arctic environment
Peak Gain	30.5 dB
Azimuth Pattern of Planar Array	
Beamwidth	2° broadside
Electronic Beam Steering	±45°
Maximum Sidelobe Level	−25 dB
Elevation Pattern (Dual Beam)	
Lower Beam Coverage	0 to 5° (nominally uniform)
Upper Beam Coverage	5 to 30° cosecant squared
Maximum Sidelobe Level	-15 dB
Phase Shifter Type	5-bit digital diode
Number of Phase Shifters	118 per face
Antenna Height	12 feet
Planar Array Width	24.1 feet
Column Network Spacing	4.9 inches
Number of Column Networks	59
Radiator Element Spacing	5.76 inches
Number of Radiator Elements	25 per column
Column Network Description	
Network Type	Center-fed tandem, stripline series feed
Height	12 feet
Depth	15 to 27 inches
Weight	13 pounds
Radiator Element Type	Folded dipole
Polarization	Vertical
Maximum VSWR	1.3
Isolation	-20 dB minimum
RF Power	500 watts peak 20 watts average
Maximum Insertion Loss	1 dB
Operating Temperature Range	-35 to 100°F

The gain and losses for the baseline antenna are itemized in table 2-2. The directivity is based upon a broadside azimuth beamwidth of 2 degrees and an elevation beamwidth of 5 degrees for the low beam. Antenna component losses are based upon expected hardware performance characteristics.

Table 2-2. Antenna Gain and Loss Budget

Directivity (dB)		35.0
Antenna Losses (dB)		
Column Network	1.0	
Diode Phase Shifters	1.2	
Azimuth Network	0.7	
Interconnecting Cables	0.3	
Quadrant Transmission Line	0.3	
Commutation Switch	1.0	
Total Losses (dB)	4.5	
Power Gain (dB)		30.5

Array phase and amplitude tolerances of 6.8 degrees rms and 0.25 dB rms, respectively, are the maximum allowable for peak azimuth sidelobes of -25 dB. The array tolerances are allocated as shown below in table 2-3.

Table 2-3. Array Tolerance Allocation

	rms Phase Error (degrees)	rms Amplitude Error (dB)
Azimuth Network	3.0	0.15
Digital Phase Shifters	5.0	0.15
Interconnecting Cables	2.5	0.10
Error Between Column Networks	2.5	0.10
	6.8	0.25

The column network phase error of 2.5 degrees rms and amplitude error of 0.1 dB rms are allocated as shown below in table 2-4.

Table 2-4. Column Network Error Allocation

	rms Phase Error (degrees)	rms Amplitude Error (dB)
Amplitude and Phase Error Between Column Networks	1.78	0.1
Transverse Position Error (±0.125 inch)	1.01	-
Axial Position Error (±0.125 inch)	1.43	-
	2.5	0.1

For -15 dB peak elevation sidelobes, the tolerance error budget within a column network is specified as follows:

a) for correlated errors: 8.2 degrees rms phase and 0.2 dB rms amplitude

b) for uncorrelated errors: 15.6 degrees rms phase and 0.4 dB rms amplitude.

2.5 BEAM POINTING ERROR FOR THE PLANAR ARRAY

An azimuth pointing error results when scanning a planar array fan beam from broadside. For the lower 5-degree beam of the baseline antenna, the azimuth error is less than 0.2° over the ±45° scan sector. For the upper fan beam, with the error normalized to zero at 15° in elevation, the maximum azimuth pointing error is typically -1.7° at 5° elevation and 3.9° at 25° elevation for ±45° of azimuth scan. The azimuth angle estimation error can be reduced by comparison of estimates from adjacent array faces. This, however, would increase the baseline array cost by requiring additional hardware to provide increased azimuth scan capability.

Because of beam characteristics, an azimuth angle estimation error results when scanning a planar array fan beam from broadside. This error is inherent to the scanning characteristics of the planar array, increasing with azimuth angle from the array normal and for increasing fan beam elevation angle. The azimuth angle error can be expressed as:

$$\alpha = \sin^{-1} [\sin \alpha_o \cos \beta_o / \cos \beta] - \alpha_o$$

where α_o is the selected azimuth angle, β is the elevation angle, and β_o is the assigned elevation angle for zero error. Figure 2-6 shows the azimuth angle error as a function of elevation angle for azimuth scan angles of α_o = 30, 45, and 60 degrees, with β_o = 0°. At an elevation angle of 20 degrees, for example, the azimuth error would be 2.1, 3.8, and 7.1 degrees for azimuth scan of 30, 45, and 60 degrees, respectively. These results would be typical for a single fan beam case and with independent planar array faces.

The azimuth angle error would be reduced for the baseline dual elevation beam system. Since the lower beam is only used over a 5° elevation range, the azimuth error would be less than 0.2° over the ±45° scan sector. The azimuth angle error is also reduced for the upper beam by adjusting for zero error at a selected elevation angle. Figure 2-7 shows the azimuth angle error normalized to zero at β_o = 15 degrees. For this case, at 30, 45, and 60 degrees of azimuth scan, the error is, respectively, -1.0, -1.7 and -2.9° at 5° elevation, and 2.2, 3.9 and 7.4° at 25° elevation.

Over limited scan regions, for the four-faced planar array, the target azimuth and elevation angles can be estimated by comparing beam information from adjacent faces to minimize the angle pointing error. For the upper beam, the resulting azimuth angle estimation error can be expressed as:

$$\alpha_{12} = (C\,\alpha_1 + \alpha_2)/(C + 1)$$

where C is a weighting coefficient dependent upon α_o and

$$\alpha_1 = \sin^{-1}\,[\sin\alpha_o \cos\,\beta_o/\cos\beta\,] - \alpha_o$$

$$\alpha_2 = \sin^{-1}\,[\sin(\,\alpha_o - 90°)\cos\,\beta_o/\cos\beta\,] - [\alpha_o - 90°]$$

By increasing the azimuth scan angle to ±60 degrees, for example, the azimuth pointing error could be reduced in the overlap region for scan angles greater than ±30 degrees. For the baseline upper beam case, the maximum error would then be described by the α_o = 30-degree curve on figure 2-7. This results in a worst case maximum error of 3.9 degrees for a target at a 30-degree elevation. Figure 2-8 shows the azimuthal error versus scan angle from broadside for various target elevation angles. This 45-degree azimuth sector provides planar array error characteristics which would be typical for the entire 360-degree scan region.

The error characteristics which have been generated represent a preliminary estimate for a four-faced planar array. Additional contributors to the beam pointing error include antenna and receiver instrumentation accuracy, clutter and multipath effects, and thermal noise limitations. The pointing error due to thermal noise on a constant amplitude target, for example, is proportional to the beamwidth and is inversely proportional to the square root of the number of samples and to the signal-to-noise level. In the cross-over region between planar array faces, the beamwidth increases and the antenna gain decreases approximately proportionally to the cosine of the scan angle, which would generally require an increased number of samples to maintain the pointing accuracy capability.

Examination of the azimuth beam pointing error for the baseline four-faced planar array indicates that the error may be reduced in the overlap region by reducing the column network spacing to provide increased azimuth scan. If, for example, each array face were designed for ±60-degree azimuth scan, then the maximum element spacing reduces to 4.435 inches. This corresponds to a 9.1 percent increase in the number of column networks for a given aperture width. A more detailed systems analysis is required to determine the allowable antenna pointing accuracy.

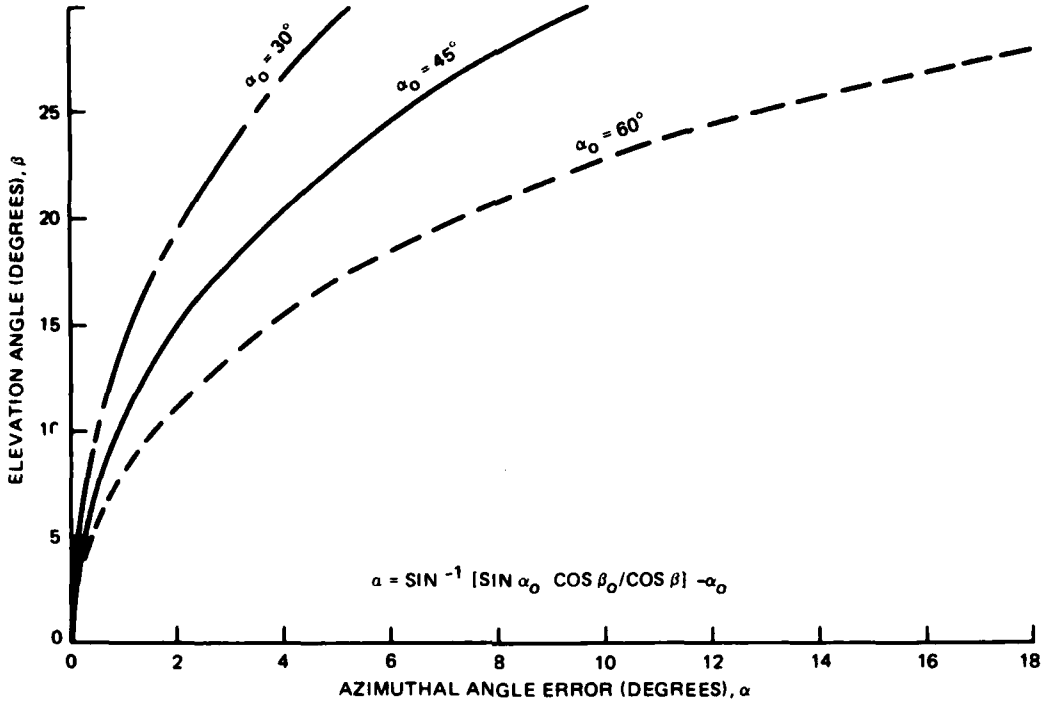

Figure 2-6. Azimuth Angle Error Versus Elevation Angle (β_o = 0 Degrees)

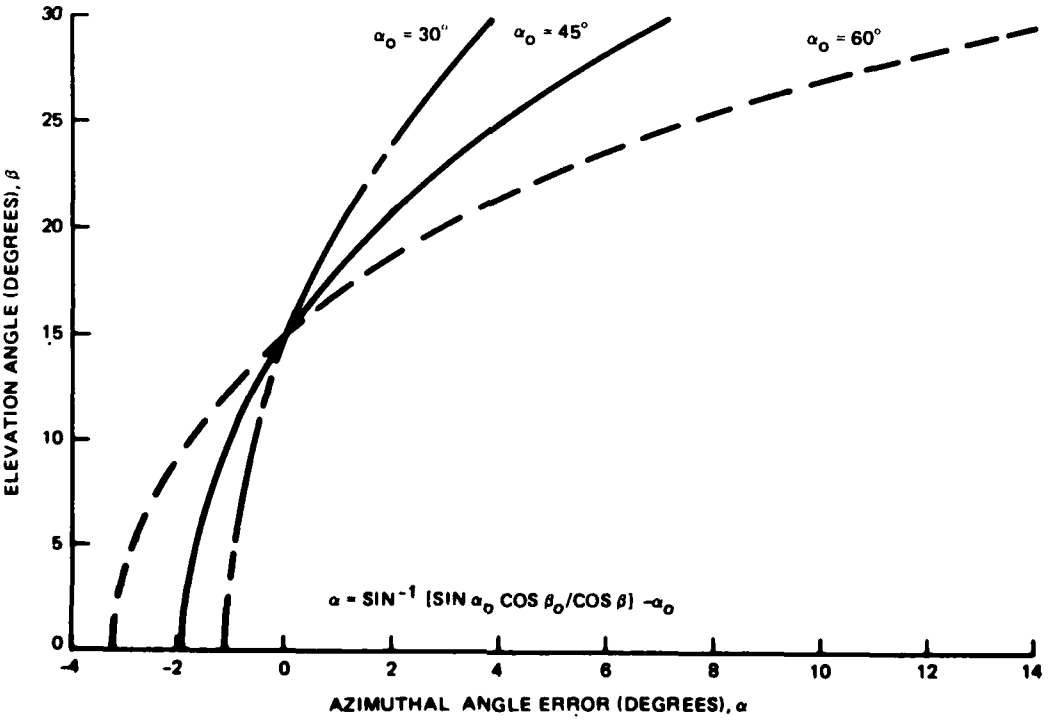

Figure 2-7. Azimuth Angle Error Versus Elevation (β_o = 15 Degrees)

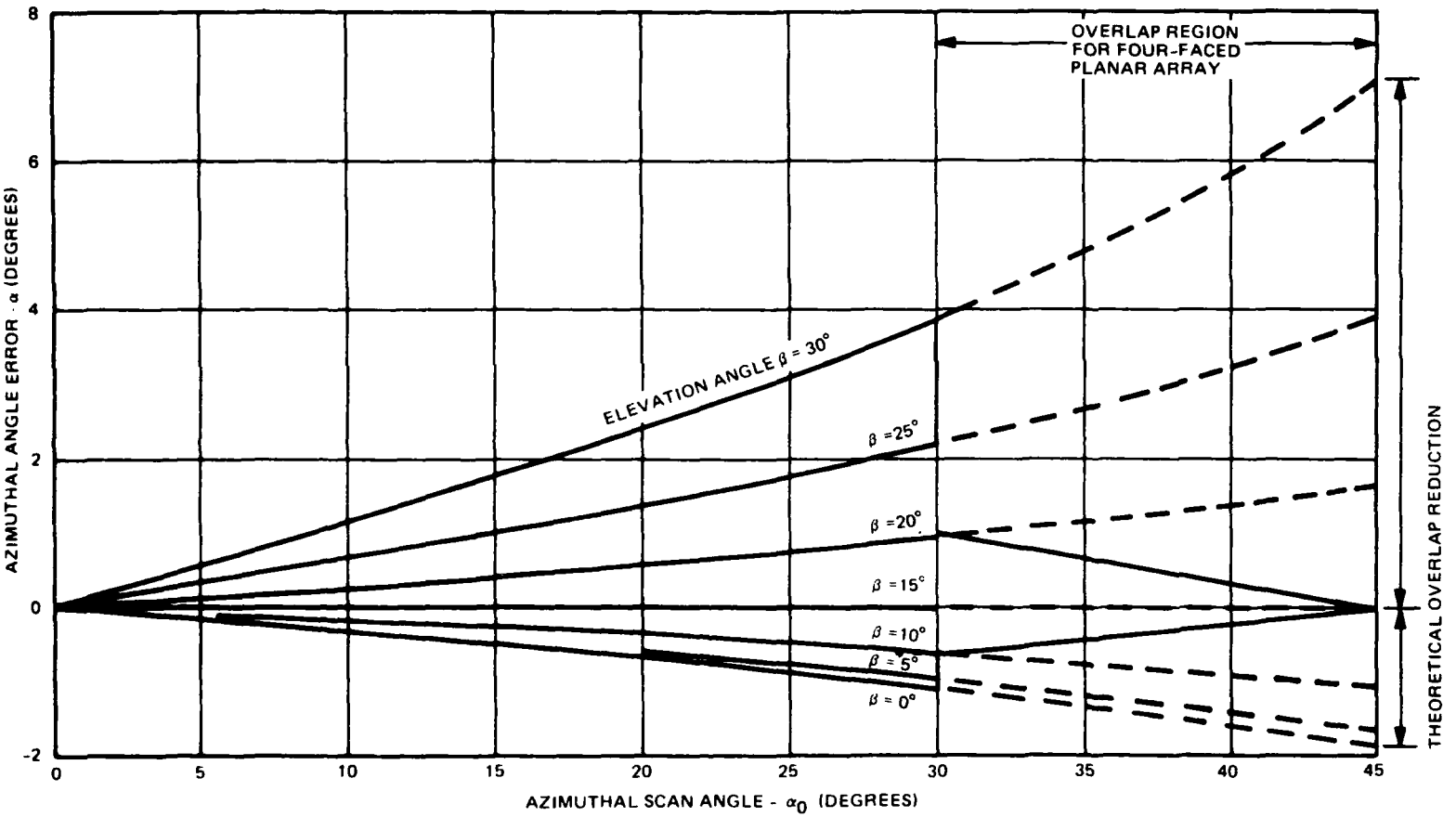

Figure 2-8. Azimuth Angle Error Versus Scan Angle (β_o = 15 Degrees)

2.6 SOLID STATE TRANSMITTER TRADE-OFF

A number of RF configurations were evaluated in detail for a solid state transmitter system. The major objective was to select a cost effective system that would provide low power consumption and high reliability. The candidate configurations consisted of locating the major power amplifiers at three different extreme locations in an antenna system with 59 column networks for each planar array face. As indicated in figure 2-9, these candidate positions included the following:

- Solid State Big Bottle - The required transmit RF power is obtained from a big bottle solid state amplifier assembly located at the input to an azimuth and elevation RF distribution system.
- Intermediate Amplifier Modules - Separate amplifier modules located at each output of an azimuth distribution network prior to SP4T sector switches. (Qty - 59).

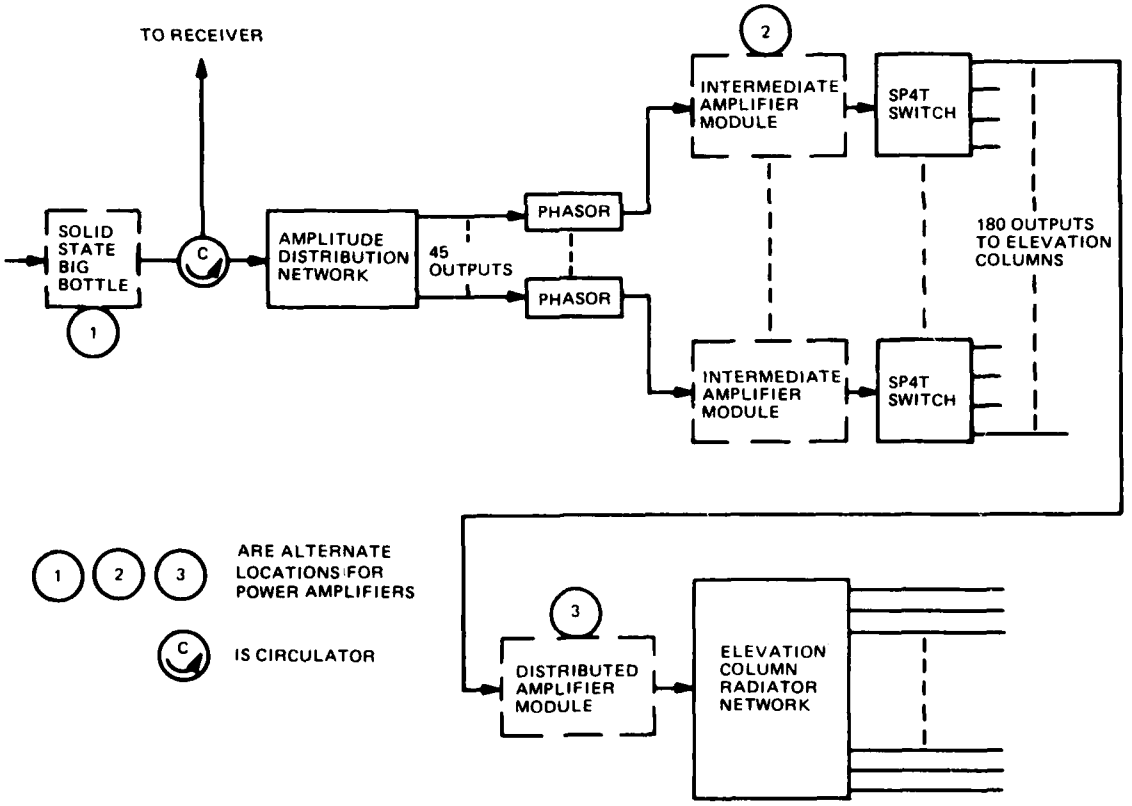

Figure 2-9. RF System with Three Alternative Locations for Power Amplifiers, Block Diagram

- Distributed Amplifier Modules - Separate amplifier modules located at the input to each column network. (Qty - 236).

The important conclusions from the trade-off investigations are:

- When the RF amplifiers are located closer to the radiating elements, the system becomes more efficient, since the amplifiers do not have to overcome the RF distribution losses.

- Amplification at the elements in a commutating planar array is more costly, since it requires more transistors and modules.

- The optimum approach will generally be a compromise between prime power consumption and implementation cost.

- A typical configuration is described using intermediate module amplifiers, located at each output of an azimuth network, for the low beam transmit signal, and a medium power solid state bottle to provide the transmit signals for the upper beam and the drive signals for the intermediate amplifiers module.

- The use of stand-by-amplifiers to replace a failed amplifier automatically is the most cost-effective means of achieving significant improvement in reliability.

The trade-off study was performed for two different radiated, RF power conditions; 2.5 kilowatts peak at 10% duty cycle, and 5.0 kilowatts peak at 7% duty cycle. Both power levels were at 100-microsecond pulsewidth. A comparison was also performed using low noise receive amplification.

One of the most important considerations for the trade-off study, was the selection of the high power transistor to be used as the basic building block for the power amplifiers. Sperry has recently completed a program for the design, fabrication, and test of an experimental 2.5-kilowatt solid state transmitter for unattended, L-band radar applications. This program was sponsored by Rome Air Development Center under contract number F30602-F-C-0245. At the outset of this program, Sperry conducted a thorough vendor search and evaluation for the latest available L-band bipolar, power transistors. This included devices from the top four suppliers, TRW, MSC, PHI, and CTC. All of the devices are grounded base transistors operating in a class C mode. As a result of this evaluation the TRW transistor was selected because of its substantial improvement in efficiency. Subsequently, TRW modified the device to Sperry specifications (improved gain) and supplied 80 devices for the 2.5-kilowatt amplifier program. This transistor (MRA-296) is rated at 100 watts output power at 100 microsecond pulse width and 10% duty cycle. For the 2.5-kilowatt amplifier program, as well as the proposed RRAS solid state transmitter system, the devices are derated a minimum of 15% to a maximum output power of 85 watts peak. This will reduce the power dissipated in the device and lower junction temperatures to conservative levels, thereby achieving high reliability operation. Reducing the transistor output power requires the use of more devices to obtain the required transmit levels. Consequentyly, the derating factor is a compromise between cost and reliability. The typical

performance for the MRA-296 transistor is presented in figure 2-10. As indicated, the minimum performance over the 1215 to 1400 MHz frequency range is 85 watts output power, 7.5 dB gain, and 52% efficiency.

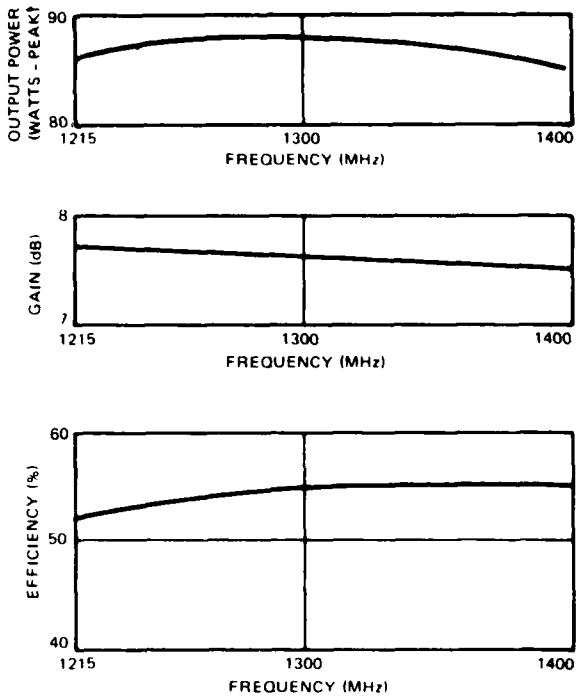

Figure 2-10. TRW MRA-296 Transistor Test Data

With the MRA-296 transistor as the basic building block, a trade-off study was performed for the three transmitter configurations previously described. The results of this investigation are summarized in comparison in table 2-5. As the RF amplifiers are located closer to the radiating elements, the transmitter system becomes more efficient and the prime power is reduced. However, amplification at the elements in a commutating planar array is more costly since it required more transistors and modules. Consequently, the optimum approach will be a compromise between prime power consumption and costs.

As a result of the above trade-off investigation, a typical solid state transmitter configuration might utilize a combination of a medium power bottle (solid state transmitter) and intermediate transmit amplifier modules with a total radiated power of 2.5 kilowatts. The solid state transmitter would provide the transmitter power for the upper beam and the drive signals for the

Table 2-5. Solid State Transmitter Comparison Results

	2.5-kilowat Transmit Power		5.0-kilowat Transmit Power	
Configuration	Relative Cost System	Prime Power (watts/sys)	Relative Cost System	Prime Power (watts/sys)
SOLID STATE BIG BOTTLE	1.0	860	1.7	1200
INTERMEDIATE MODULE				
• W-LNA	1.9	370	3.0	550
• W/O-LNA	1.6	600	2.5	740
DISTRIBUTED MODULE				
• W-LNA	4.0	250	-	-
• W/O-LNA	3.6	430	-	-

transmit amplifier modules. The final amplification for the low beam transmit signal is provided by the transmit amplifier modules located in each output of an azimuth distribution network.

The anticipated performance and parameters for the solid state transmitter and transmit amplifier modules are as follows:

	Solid State Transmitter	Transmit Amplifier Modules (45)
Output Power (watts, peak)	450	2330 (total)*
Gain (dB)	26.5	17
Efficiency	37%	42%
Vcc	28v/32v	28v
Prime Power (watts, avg) (10% DC)	120	560
MTTR (replace spare module)	1/2 hr	1/2 hr
Size (inches)	12 x 8 x 6	60 x 12 x 6
Weight (lbs)	10	80

*Includes amplitude tapering effect.

A block diagram for a typical solid state transmitter is presented in figure 2-11. It consists of a driver module with two identical 3-stage amplifier channels connected at their input and output by a SPDT diode switch. One of the channels is a standby unit that is automatically switched into the circuit when there is a failure to the operating channel. The output from the driver module is distributed equally to 6 of the 7 paralleled output stage transistors, through a 1P6T power divider/switch network. The 7th output transistor amplifier is a standby unit that is automatically switched into the circuit when there is a failure to any of the 6 operating amplifiers. The output power from the 6 operating transistors is efficiently combined in an identical 1P6T power combiner/switch network. These networks are stripline, center fed, reactive, power dividers with shunt mounted diodes in each of the 7 output arms located a quarter wavelength from the center junction. The input signal can be distributed equally to any 6 of the 7 output with the proper biasing of the diodes. With 1-watt peak RF input power, the solid state transmitter will provide 450 watts peak output power at a collector voltage of 31 volts. About 370 watts will be used for the upper beam and the remainder (80 watts) to drive the 59 transmit amplifier modules for the low beam.

This concept of self-healing, using stand-by amplifiers that automatically replace failed units, has been demonstrated by Sperry during the acceptance tests of the 2.5-kilowatt solid state, L-band transmitter developed for RADC. Reliability calculations for the RADC program indicated 2 orders of magnitude improvement in reliability with the use of one standby module. Consequently, this technique of self-healing is a practical, cost-effective approach for obtaining significant improvement in reliability.

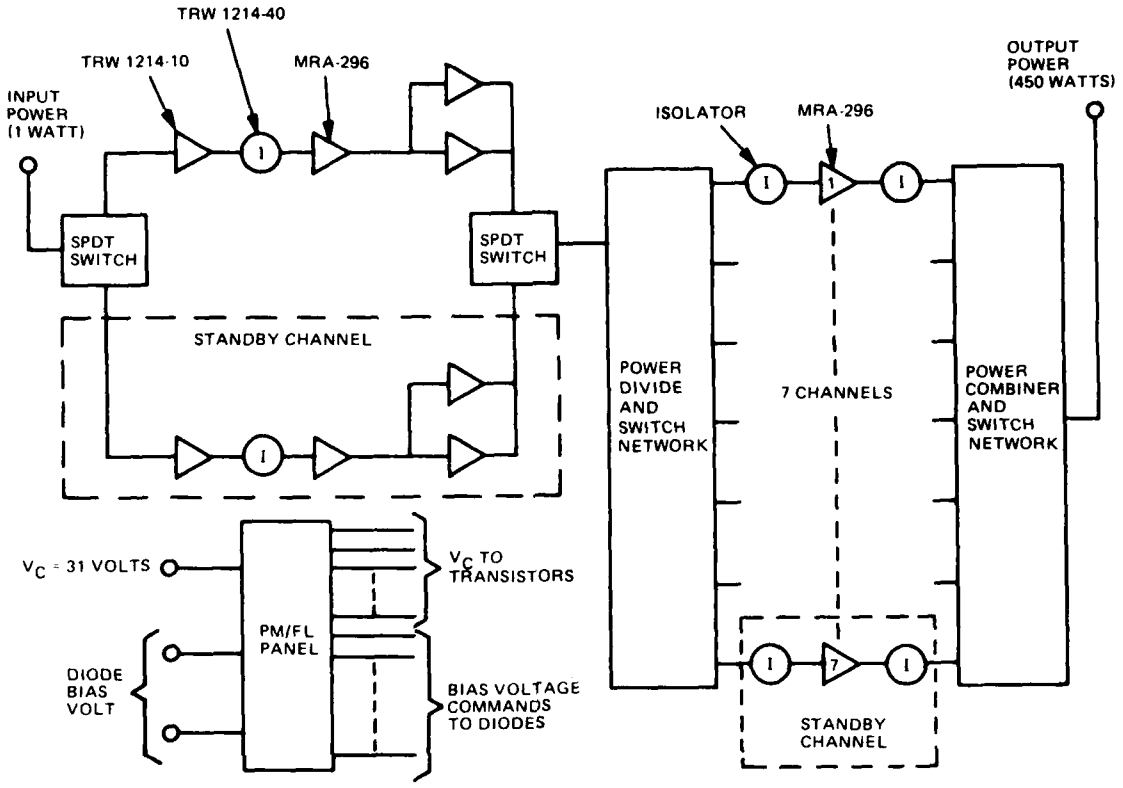

Figure 2-11. Solid State Transmitter, Block Diagram

A performance monitoring and fault locating (PM/FL) panel will be used to provide the sensing, logic, and switching circuits needed to monitor the transistor collector currents and automatically replace a failed amplifier with a standby unit.

A block diagram of the 59 transmit amplifier modules for the low beam signal is presented in figure 2-12. Each of the identical amplifier channels contain three stages of amplification and a duplexer to separate the transmit and receive signals. The duplexer consists of a circulator and a SPDT diode switch arrangement. This configuration efficiently separates the transmit and receive signals, and it also converts the circulator at the output of the module to an isolator during the transmit mode. This protects the output stage from antenna load variations.

The maximum RF transmit output power from any one of the 59 amplifier modules is about 110 watts peak with 1 watt RF input and a collector voltage of 31 volts. This RF output power must be reduced from the maximum value for a range of about 13 dB to provide the desired azimuth illumination taper for sidelobe control. This will be accomplished by reducing the collector supply

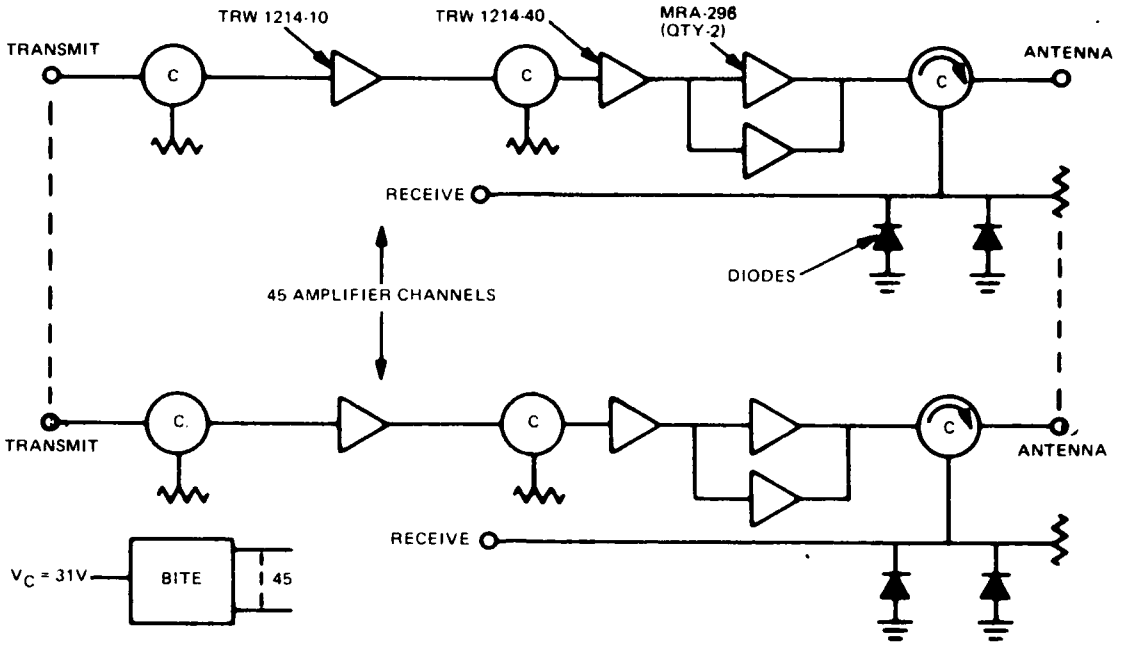

Figure 2-12. Transmit Amplifier Module, Block Diagram

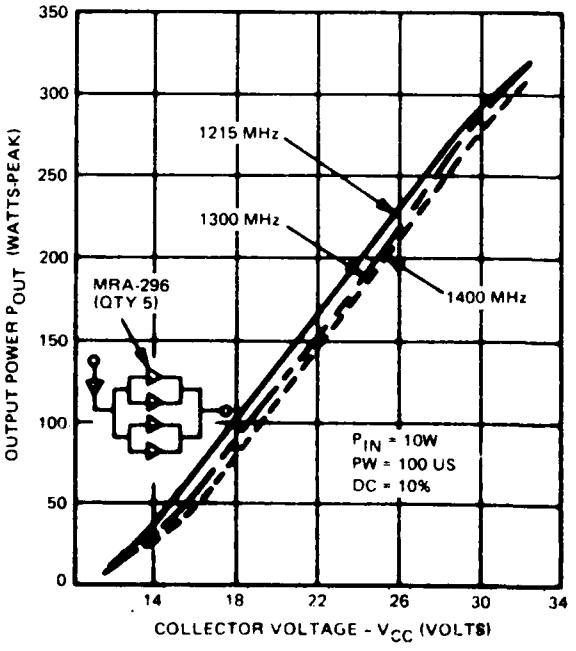

Figure 2-13. Breadboard Module Test Data

voltages where necessary. A typical amplifier response for the output power variation, as a function of a collector voltage, is presented in figure 2-13. The test data are for a two-stage amplifier module, using the MRA-296 transistors, developed for the 2.5-kilowatt L-band amplifier for RADC. As indicated, there is a fairly linear 13 dB reduction of output power as the collector voltage is reduced from 32 volts to 12 volts. Since the proposed transmit amplifier modules contain three stages of amplification, a smaller voltage reduction will be required for the 13 dB output power reduction.

The concept of graceful degradation can be applied for the 59 separate transmit amplifier modules. When one of the transistors fail, the loss of that channel will not seriously affect the array performance. As a result, it is not necessary to use standby amplifiers to achieve the required reliability.

Section 3

DESIGN, FABRICATION, AND TESTING OF A DUAL BEAM COLUMN NETWORK

3.1 TASK SUMMARY

This section describes the design and fabrication of a stripline dual beam column network. The task was to build a stripline network which demonstrates both the feasibility of manufacturing a large stripline network and the achievable electrical performance of this network.

3.2 NETWORK DESIGN AND FABRICATION

The unattended radar requires two simultaneous beams - a lower pencil beam and an upper csc^2 fan beam. A dual beam network forming simultaneous pencil and csc^2 beams was designed, built, and tested during this program. The network, described in this section and shown in figure 3-1, is a low loss, single-layer stripline, center-fed, tandem series network which generates two completely independent array excitations corresponding to the two elevation beams. The network forms the beams over a broadband (1.2 to 1.4 GHz) with low loss (1.05 dB). It excites a set of printed stripline dipoles which are the vertically polarized radiating elements of the array.

To satisfy the dual shaped beam requirements while still maintaining minimum loss in the feed network, each beam excitation is selected from sets of orthogonal beams employing complex weights. In developing the two elevation beam excitations, a modified Woodward synthesis procedure (1) was followed employing complex weights for orthogonal beams to generate the desired beam shape.

The utilization of complex weights between orthogonal beams provides reduction of the shaped beam ripple, as well as some control over the sidelobe level. By using orthogonal beams for synthesizing both excitations, the resultant shaped beams are then orthogonal, enabling their theoretical lossless generation via a distribution network such as the dual channel, center-fed series network proposed by Sperry.

In synthesizing the beam excitations, a high degree of flexibility exists. However, to satisfy the network and antenna performance requirements, the synthesis and beam selection procedure utilized had to satisfy a specific set of constraints. The flexibility of the approach, as well as the results of applying the design constraints, is explained as follows.

- - - - - - -

(1) Woodward, P.M., "A Method of Calculating the Field Over a Plane Aperture Required to Produce a Given Polar Diagram," IEEE (London) Part III, Vol. 93, 1947, 1554-1558.

Figure 3-1. Dual Beam Network

In general, for an array of N elements, N-1 orthogonal beams exist in the spatial region between grating lobe positions. Consider the case where the array elements are spaced $\lambda/2$ apart. The set of orthogonal beams would span all of real space. Increasing the element spacing has the effect of decreasing the grating-lobe-free scanable spatial region accordingly. Keeping the number of elements constant, as the array spacing is increased, has the effect of "pulling-in" the set of orthogonal beams to a narrower spatial region. This is illustrated in figure 3-2. The first set of orthogonal beams represents an array of 10 elements spaced $\lambda/2$ apart. The second set of beams shows what happens when the array element spacing is increased to $2\lambda/3$. The beams narrow and gain increases because of the resultant larger array aperture. The orthogonal beams are pulled closer together at the expense of reducing the scan coverage. However, by spacing the elements as far apart as tolerable, the aperture gain is maximized with a minimum number of elements. These conditions have been incorporated into the dual beam selection procedure in the proposed baseline design.

Once the array is sized and the element spacing is selected, a beam synthesis procedure is followed to develop the two shaped beam excitations. This results in an ideally lossless network with the two shaped beams being orthogonal. Since only N-1 orthogonal beams are available to synthesize the shaped beams, the first task in either approach is to determine which beams are to be used for forming each of the two shaped beams. The orthogonal beams which are used to generate one beam excitation cannot be used to generate the other beam excitation. This results in two shaped beam excitations which are orthogonal and easily generated via an ideally lossless network.

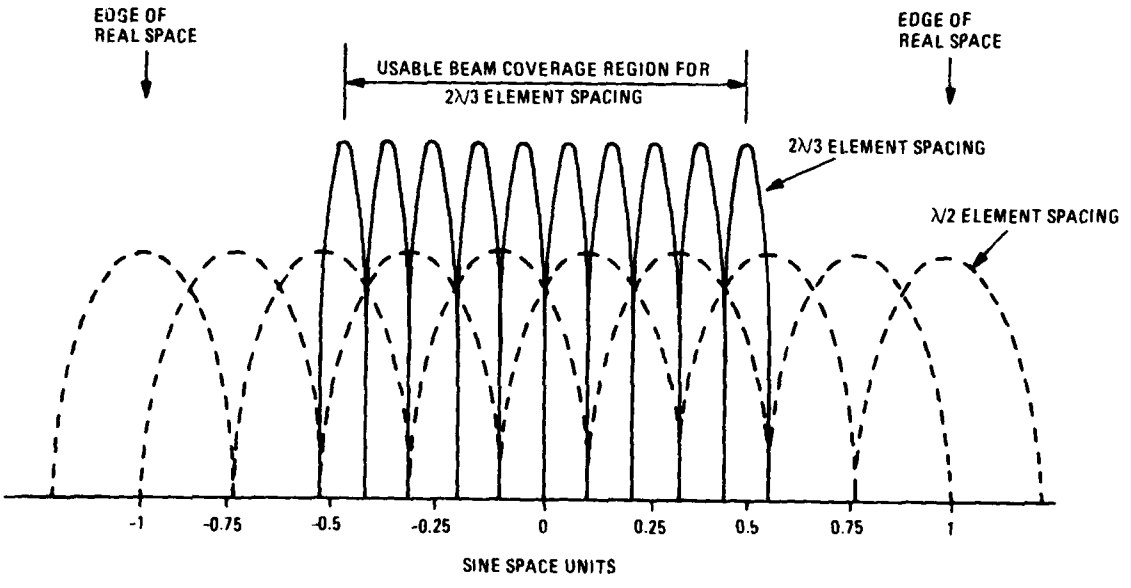

Figure 3-2. Orthogonal Beam Sets for $\lambda/2$ and $2\lambda/3$ Element Spacings

Imposing the constraint that the feed network is ideally lossless necessitates the utilization of separate orthogonal beams in the synthesis of the two elevation beam excitations. Based on the coverage requirements and grating lobe conditions, a 12-foot elevation aperture size and 5.76-inch interelement spacing was selected. This results in a 0.063 sine space unit spacing between orthogonal beams, which corresponds to approximately 3.61 degrees between beams near broadside at mid frequency (1.3 GHz). To meet the low elevation beam requirement of uniform gain from 0 to 5 degrees with rapid field drop-off beyond the coverage region, a trade-off study was performed using two and three orthogonal beams to shape the low elevation beam. The results showed that while a flatter beam shape could be obtained using three orthogonal beams, greater gain and a sharper main beam drop-off is obtained using two orthogonal beams - hence providing superior antenna performance. Typical results for the two cases are plotted in figure 3-3. Note that both patterns have the same gain at 0 and 5 degrees, but that the beam synthesized with two orthogonal beams has greater gain over the coverage region, being 1.8 dB more at the beam peak and a sharper drop-off outside the coverage region. This represents significantly superior antenna performance, and therefore a two-beam synthesis was chosen for the lower beam.

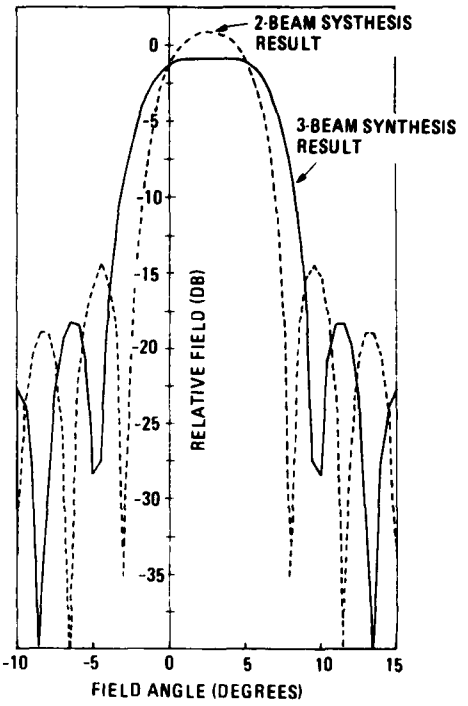

Figure 3-3. Comparison of Low Elevation Beams with Two and Three Orthogonal Beam Syntheses

The upper elevation beam with a cosecant squared gain drop-off was then synthesized using seven orthogonal beams, none of which were used for the low elevation beam synthesis. In both cases, complex weighting of the orthogonal beams was utilized to generate the two composite beams.

A typical set of results is displayed in figure 3-4. Both the upper and lower elevation beams computed at center frequency are plotted. In both cases, the beam shapes were optimized with a constraint that the sidelobe level not exceed 15 dB below the peak gain while maintaining orthogonality between beams. The excitations for these beams can therefore be generated via a dual channel series feed network which is ideally lossless. Also plotted in figure 3-4 is a cosecant squared gain drop-off from 5 to 30 degrees above the horizon. This gain drop-off is shown relative to the lower beam value at 5 degrees. The network designed and built during this study is based on this two-beam synthesis for the lower beam and a seven-beam synthesis for the upper beam.

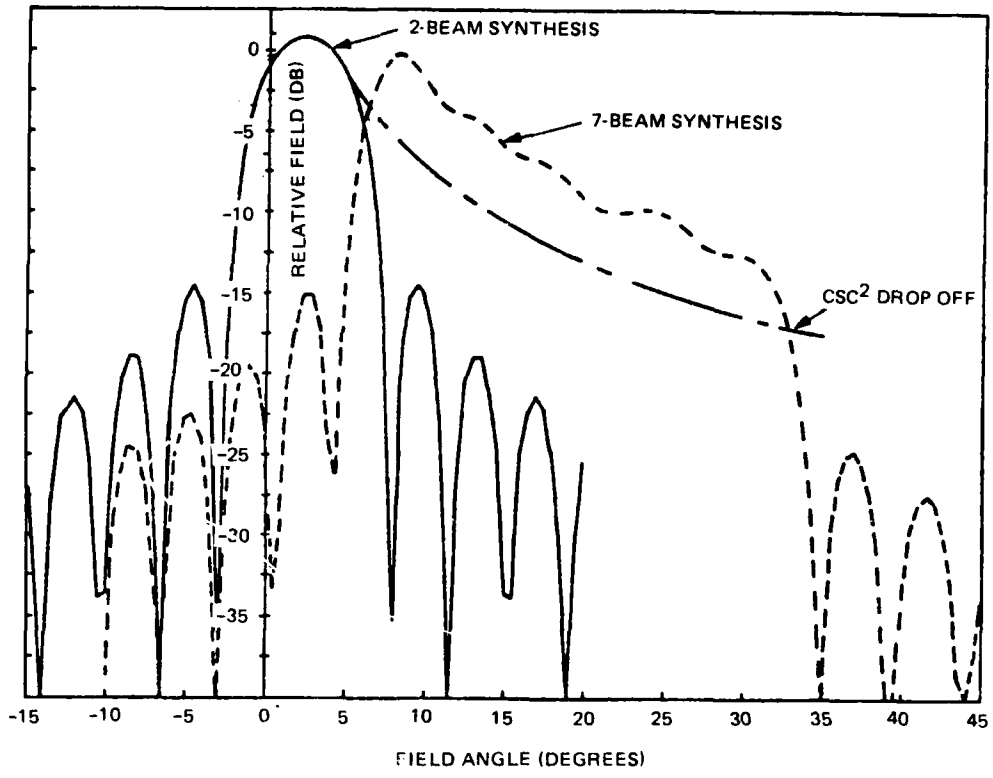

Figure 3-4. Dual Shaped Orthogonal Beams (Theoretical Curves)

A layout of the printed circuit, including the radiating dipoles, is shown in figure 3-5. The design consists of a stripline dual channel series network and radiating dipoles printed on a single, foam supported circuit. The design is simple, economical, and lightweight. The use of separate components and interconnecting cables is avoided, because cables and interconnections are expensive and unreliable, and also contribute to increased loss.

The photograph of the final breadboard shown in figure 3-1 has the upper ground plane and dielectric removed to show the printed circuit stripline. For this breadboard, the radiating dipoles have been cut off and replaced by type N coaxial connectors to permit the measurement of the amplitude and phase at each output. The circuit is shown schematically in figure 3-6. The network produces two orthogonal illumination functions for the upper csc^2 beam and the lower pencil beam, with no loss into the network terminations. The orthogonal illumination functions are formed by the appropriate choice of coupling values and appropriate phase adjustments. In the network, the lower beam amplitudes

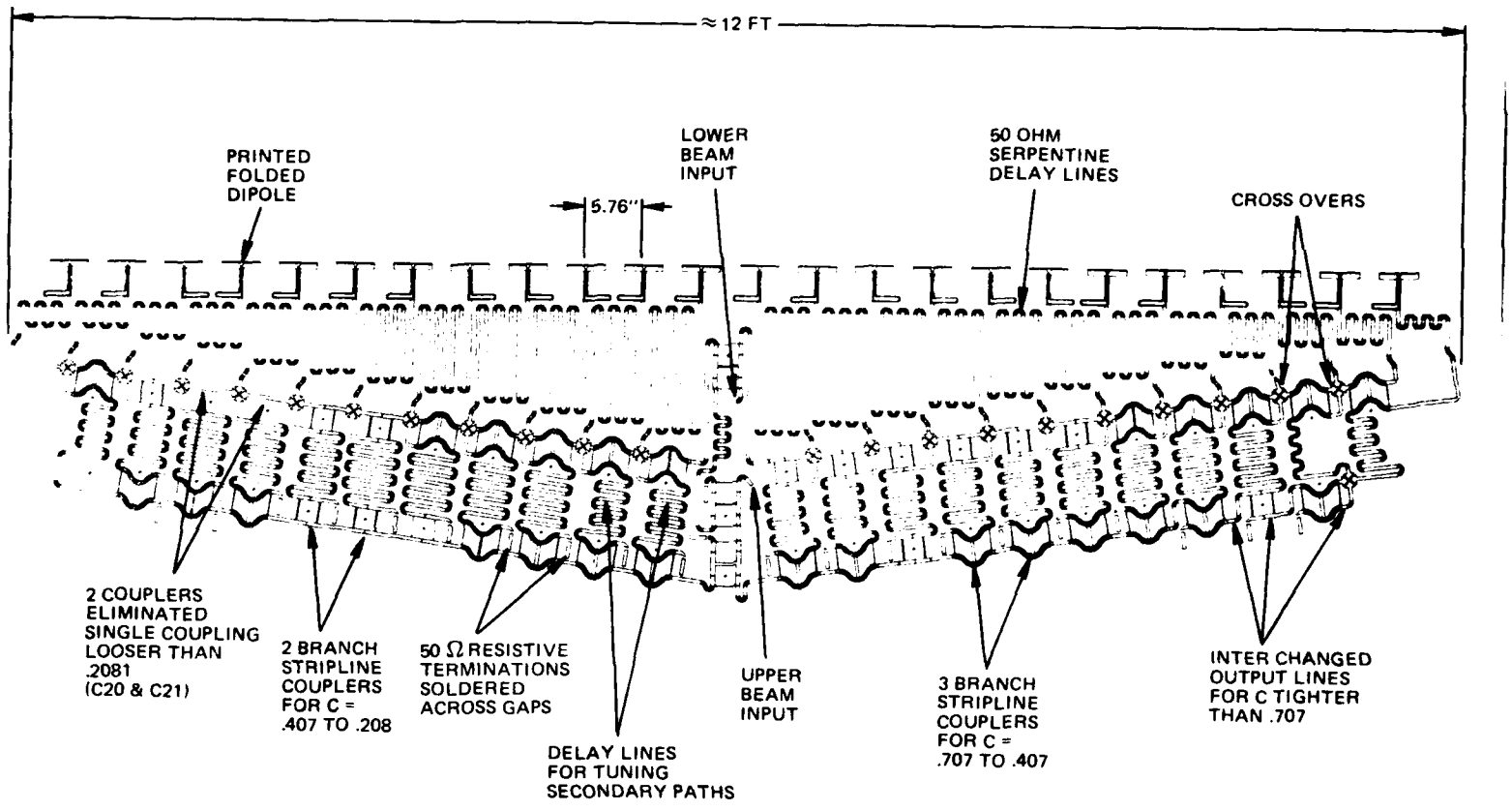

Figure 3-5. Computer-Aided-Design of Network Layout

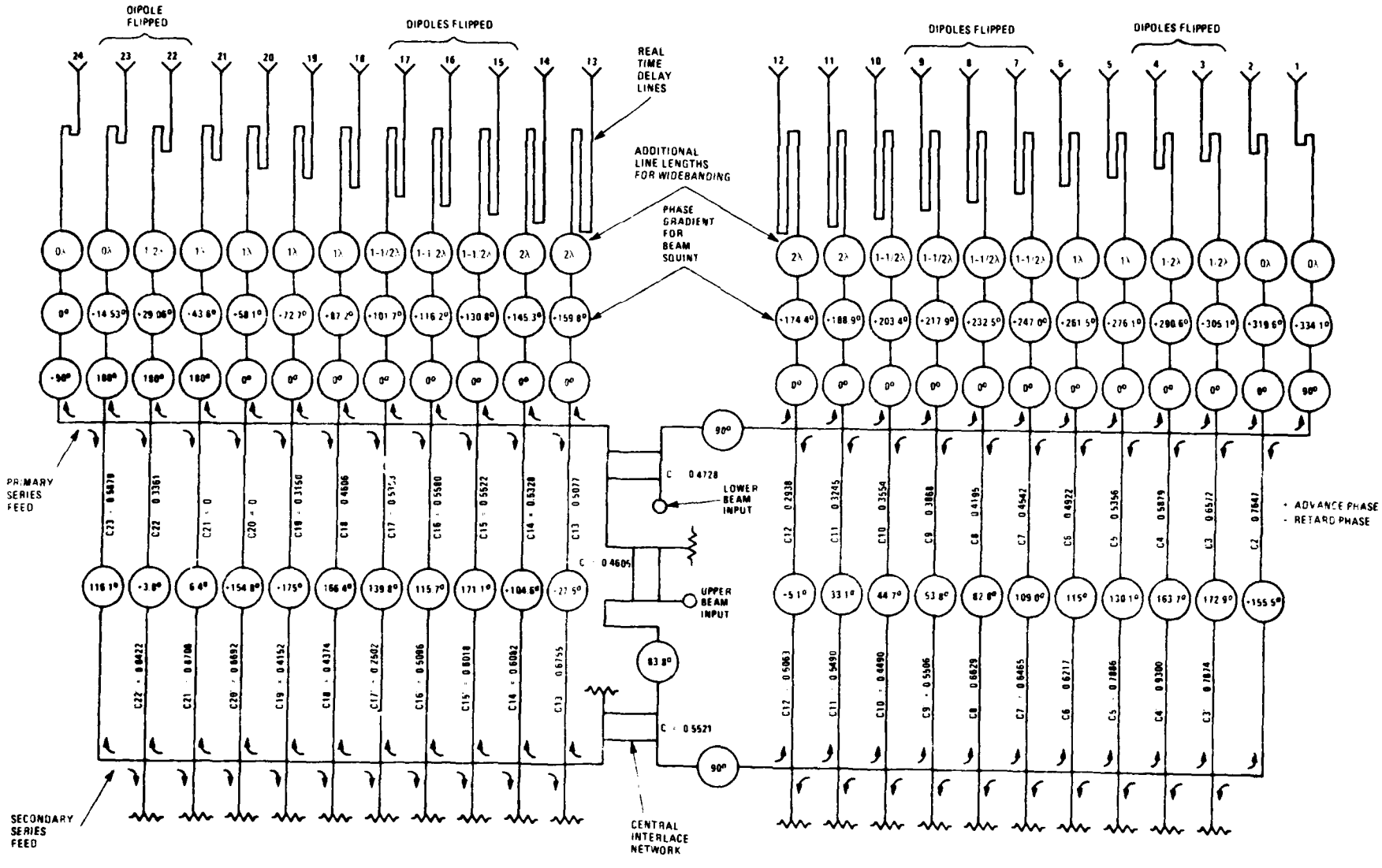

Figure 3-6. Network Design, Schematic Diagram

are determined only by the couplers in the primary series feed (C2 thru C23) and the network shown in the schematic is theoretically lossless because the final outputs to elements 1 and 24 are coupled directly to the radiator. The lower beam phases are determined by line length adjustments in the real time delay lines.

The amplitude and phases for the upper cosecant squared beam are formed by a combination of the primary and secondary series feeds. The central interlace network provides the required distribution of energy between the primary and secondary series feeds. The design of the network involves the computation of multi-path vectors through the primary and secondary lines. Both the upper and lower beams are formed simultaneously and are theoretically lossless because the illumination functions are orthogonal.

Real time delay lines are provided on the outputs to equalize the path lengths between the input and each of the 24 outputs. This permits the circuit to operate broadband (1.2 to 1.4 GHz) without defocusing. However, the path lengths are not all physically equal. As can be seen in the schematic, the central paths (elements 11, 12, 13, and 14) have an additional two wavelengths of path length over and above the end elements (1, 2, 23, and 24). Elements 7, 8, 9, 10, 15, 16, and 17 have an additional 1½ wavelengths; elements 5, 6, 18, 19, 20, and 21 have an additional 1 wavelength; and elements 3, 4, and 22 have an additional ½ wavelength. This was necessary to compensate for the phase response of the directional couplers in the series feed. The insertion phase of a directional coupler does not exactly follow that of a transmission line. At center band, where the coupling branches and separations are exactly one quarter wavelength long, the insertion phase of a coupler is exactly equal to that of an equal length of uncoupled line, regardless of its coupling value. Thus, a two-branch coupler is 90 degrees long, and a three-branch coupler is 180 degrees long. However, the insertion phase slope is a function of its coupling value. An uncoupled length of TEM line has an insertion phase linearly dependent on the operating frequency. A coupler has a slope greater than that of an uncoupled line, and the tighter the coupler, the greater the slope. The insertion phase slope of each of the couplers in the network was calculated by computer analysis, and the additional multiples of ½ wavelength have been added to compensate. The end elements pass through more couplers than the central elements, and therefore have a greater phase slope than the central elements. The phase slope across the 24 elements is equalized by adjusting line lengths between coupler and output port in multiples of ½ wavelength as the phase slope accumulates from the center to the outer elements. Every time an additional ½ wavelength of line length is added, the phase of the radiated energy is recorrected by flipping the dipoles. In addition, a phase gradient is applied to the outputs in order to squint the peak of the lower beam 3.65 degrees below the array normal. The array normal is tilted 6 degrees above the horizon, so that the lower beam peak will be 2.35 degrees above the horizon to provide the proper coverage. The phase tilt also eliminates a grating lobe on the upper fan beam.

It should be noted that the illuminations are not symmetric about the center, and the coupling values and phases are not symmetric. The main reason for center feeding the network was to minimize the line length from the input

to each of the 24 outputs in order to minimize I^2R loss. The I^2R loss of the transmission lines is minimized by building the network in stripline supported by low loss, foam dielectric and by minimizing the length of the stripline network. At 1.3 GHz, the total measured insertion loss of the final network shown in the photograph is 1.3 dB for both the lower beam channel and the upper beam channel, including 3 feet of 0.141 semi-rigid coax cable on each of the inputs (used for measurement ease) which accounts for approximately 0.25 dB of this loss. The network loss is therefore 1.05 dB. This measurement was made by integrating the power output of the 24 ports and comparing it to the input power to the lower or upper beam inputs. This is in close agreement to the specified 1 dB goal. Detailed summaries of the measured amplitudes and phases are given in tables 3-1 through 3-4. The calculated antenna patterns using the measured phase and amplitude outputs are given in figures 3-7 through 3-10.

The stripline construction consists of transmission lines etched on 0.003-inch Kapton sheets with 0.0014-inch thick copper cladding on one side. The ground plane spacing of 0.250 inch is determined by sandwiching the circuit between two 0.125-inch thick dielectric sheets consisting of Emerson and Cummings PP as described in subsection 4.2. (See figure 4-1). Thin aluminum sheets form the outer ground planes. However, the network could also be built in any of the stripline configurations described in section 4.2. No redesign of the stripline printed circuit would be necessary since it is essentially a very broadband real time network, and it would work even if the dielectric constant were changed slightly. This permits the substitution of HEXCEL or polyurethane, for the Emerson and Cumming PP presently used. Table 4-4 in Section 4 presents measured values of the effective dielectric constant with various combinations of dielectric and PC substrates. The maximum variation in wavelength is 3 percent, but the network operates over a 15 percent band, and therefore any of these combinations are usable if the increased I^2R loss can be tolerated.

The procedure used to print the network involved Computer-Aided-Design (CAD). A layout of the full printed circuit stripline network was generated and stored in the computer aided design machine. Figure 3-5 is a reduced scale print of the completed layout as plotted by the CAD machine. The actual full scale printed circuit, figure 3-1, is 12 feet in length. The information from the CAD machine was translated into commands to control a large and extremely accurate Gerber X-Y plotter carrying a light pen. The Gerber plotter and light pen exposed large sheets of photographic film, automatically generating full size photo-mask negatives of the stripline circuitry. The photo-masks were used for contact exposure of photo resist coating in the etching process of the stripline circuits. Prior to this program, negatives for microwave stripline circuits were generally cut by hand on Rubylith with the aid of a coordinagraph. The circuits were cut on an enlarged scale and photo-reduced for accuracy. However, the unattended radar dual beam column network is so large and complex that it required working out this computer-aided technique to plot the negatives automatically. The technique was also used recently, with excellent results, in the production of 30 similar stripline networks for a large phased array.

The final network shown in figure 3-1 was made from five sheets of Kapton, each 2 feet by 3 feet. Patching is a simple process requiring only two overlapping solder joints between two adjacent sheets. Printing larger sheets was impractical due to a limitation on the size of the Kapton material. Although this material is available in the form of long rolls, it was found that roll Kapton shrinks considerably after the etching process. Flat sheet Kapton, which was used to build the breadboard, does not shrink, but is not available in

Table 3-1. Measured Lower Beam Amplitudes

N	dB Theoretical (plus 1.3 dB I^2R)	dB Measured			dB Error		
		1.2GHz	1.3GHz	1.4GHz	1.2GHz	1.3GHz	1.4GHz
1	-17.20	-18	-18.3	-19.4	-0.8	-1.1	-2.2
2	-15.71	-17.1	-16.9	-18.2	-1.4	-1.2	-2.5
3	-14.57	-15.3	-15.6	-16.4	-0.7	-1.0	-1.8
4	-13.69	-14.2	-14.3	-14.9	-0.5	-0.6	-1.2
5	-13.04	-13.4	-13.5	-13.8	-0.4	-0.5	-0.8
6	-12.57	-13.2	-13	-13.3	-0.6	-0.4	-0.7
7	-12.26	-12.6	-12.5	-12.8	-0.3	-0.2	-0.5
8	-12.11	-12.2	-12.2	-12.9	-0.1	-0.1	-0.8
9	-12.11	-11.7	-12	-12.1	+0.4	+0.1	0
10	-12.26	-11.7	-11.8	-11.8	+0.6	+0.5	+0.5
11	-11.34	-12	-12	-12	-0.7	-0.7	-0.7
12	-13.04	-12.3	-12.2	-12	+0.7	+0.8	+1.0
13	-13.69	-13.1	-13.2	-12.9	+0.6	+0.5	+0.8
14	-14.57	-13.7	-14	-14	+0.9	+0.6	+0.6
15	-15.71	-15.2	-15.5	-15.8	+0.5	+0.2	-0.1
16	-17.20	-16.9	-17	-17.3	+0.3	+0.2	-0.1
17	-19.20	-19	-19.6	-19.6	+0.2	-0.4	-0.4
18	-21.95	-21.8	-21.9	-22.1	+0.2	+0.1	-0.2
19	-26.27	-26.6	-25.8	-26.9	-0.3	+0.5	-0.6
20	$-\infty$	-45.5	-41.2	-41.6	Leak	Leak	Leak
21	$-\infty$	-41	-44.5	-40.8	Leak	Leak	Leak
22	-26.29	-25.9	-25.9	-26.9	+0.4	+0.4	-0.6
23	-21.95	-22.2	-22.8	-22.7	-0.3	-0.9	-0.8
24	-19.18	-19.9	-20.2	-21	-0.7	-1.0	-1.8

	1.2GHz	1.3GHz	1.4GHz	
Integrated Power (Σ_p)	0.751	0.737	0.699	
I^2R Loss (dB)	-1.241	-1.325	-1.567	- (Includes 0.25dB loss for 3 feet 0.141 coax on input)

Table 3-2. Measured Upper Beam Amplitudes

N	dB Theoretical (plus 1.3 dB I^2R)	dB Measured			dB Error		
		1.2GHz	1.3GHz	1.4GHz	1.2GHz	1.3GHz	1.4GHz
1	-20.51	-20.6	-21.5	-22.9	-0.1	-1.0	-2.4
2	-21.46	-20.9	-23.5	-26.6	+0.6	-2.0	-5.0
3	-18.49	-17.2	-19.8	-23.7	+1.3	-1.3	-5.2
4	-16.51	-15.2	-16.7	-18.9	+1.3	-0.2	-2.4
5	-16.85	-16.8	-17.0	-18.0	+0.1	-0.2	-1.2
6	-16.97	-16.6	-16.9	-18.1	+0.4	+0.1	-1.1
7	-14.77	-14.4	-14.4	-14.9	+0.4	+0.4	-0.1
8	-13.61	-14.3	-13.7	-13.9	-0.7	-0.1	-0.3
9	-14.68	-16.0	-15.0	-15.5	-1.3	-0.3	-0.8
10	-14.92	-16.3	-14.9	-14.4	-1.4	0	+0.5
11	-11.34	-12.1	-11.4	-11.0	-0.8	-0.1	+0.3
12	-8.81	-9.1	-9.0	-8.6	-0.3	-0.2	+0.2
13	-8.53	-7.4	-8.1	-8.6	+1.1	+0.4	-0.1
14	-10.65	-10.8	-10.5	-9.9	-0.2	+0.2	+0.8
15	-16.07	-18.8	-16.4	-14.4	-2.7	-0.3	+1.7
16	-31.13	-30.3	-32.0	-25.5	+0.8	-0.9	+5.6
17	-26.69	-25.9	-26.7	-28.2	+0.8	0	-1.5
18	-25.39	-26.7	-26.0	-25.1	-1.31	-0.6	+0.3
19	-25.66	-23.0	-25.3	-29.2	+2.7	+0.4	-3.5
20	-21.33	-22.1	-22.2	-22.1	-0.8	-0.9	-0.8
21	-20.15	-21.6	-20.7	-21.1	-1.5	-0.6	-1.0
22	-21.73	-20.9	-20.9	-21.7	+0.8	+0.8	0
23	-21.68	-20.8	-21.1	-21.9	+0.9	+0.6	-0.2
24	-19.94	-19.5	-20.2	-21.6	+0.4	-0.3	-1.7

	1.2GHz	1.3GHz	1.4GHz	
Integrated Power (Σ_p)	0.745	0.740	0.719	
I^2R Loss (dB)	-1.277	-1.307	-1.435	- (Includes 0.25dB loss for 3 feet 0.141 coax on input)

Table 3-3. Measured Lower Beam Phases (in degrees)

N	1.2GHz			1.3GHz			1.4GHz		
	Theoretical Phase	Measured Phase	Phase Error	Theoretical Phase	Measured Phase	Phase Error	Theoretical Phase	Measured Phase	Phase Error
1	154.24	150.7	3.5	7.3	11.5	-4.2	179.95	182.8	- 2.9
2	140.83	139.7	1.12	- 7.23	- 10.5	3.3	164.3	153.8	10.5
3	127.42	135.7	-8.3	- 21.76	- 19.5	-2.2	148.65	147.8	0.9
4	114.01	115.7	-1.7	- 36.29	- 30.5	-5.8	133.01	137.8	- 4.8
5	100.52	103.7	-3.2	- 50.82	- 50.5	-0.3	117.36	109.8	7.6
6	87.18	85.7	1.5	- 65.35	- 63.5	-1.8	101.71	103.8	- 2.1
7	73.77	83.7	-9.9	- 79.88	- 77.5	-2.35	86.06	79.8	6.3
8	60.36	65.7	-5.4	- 94.41	- 94.5	0.1	70.42	66.8	3.6
9	46.94	45.7	1.2	-108.94	-109.5	0.6	54.77	51.8	3.0
10	33.53	26.7	6.8	-123.47	-121.5	-1.9	39.12	43.8	- 4.7
11	20.12	24.7	-4.6	-138.0	-137.5	-0.5	23.47	18.8	4.7
12	6.71	6.7	0	-152.53	-152.5	0	7.82	7.8	0
13	- 6.71	- 6.3	-0.4	-167.06	-161.5	-5.5	- 7.82	0.8	- 8.6
14	-20.12	-17.3	-2.8	-181.59	-179.5	-2.1	-23.47	-23.2	- 0.3
15	-33.53	-40.3	6.8	163.88	164.5	-0.6	-39.12	-36.2	- 2.9
16	-46.94	-45.3	-1.7	149.35	149.5	-0.2	-54.77	-55.2	- 0.4
17	-60.36	-55.3	-5.1	134.82	141.5	-6.68	-70.42	-72.2	- 1.8
18	-73.77	-76.3	2.5	120.29	122.5	-2.21	-86.06	-83.2	- 2.9
19	-87.18	-90.3	3.11	105.76	108.5	-2.74	-101.71	-103.2	- 1.5
20	-	-	-		-	-	-	-	-
21	-	-	-	-	-	-	-	-	-
22	52.58	50.7	1.9	242.17	240.5	1.67	31.35	21.8	9.6
23	39.17	29.7	9.5	227.64	227.5	0.1	15.7	12.8	2.8
24	25.76	27.7	-2.0	213.11	219.5	-6.4	0.05	- 3.2	3.25

Table 3-4. Measured Upper Beam Phases (in degrees)

N	1.2GHz			1.3GHz			1.4GHz		
	Theoretical Phase	Measured Phase	Phase Error	Theoretical Phase	Measured Phase	Phase Error	Theoretical Phase	Measured Phase	Phase Error
1	36.19	61.5	-25.28	61.89	60.9	1.01	87.59	68.3	19.3
2	30.70	64.5	-33.77	55.29	56.9	-1.59	79.87	38.3	-41.6
3	29.59	54.5	-24.88	53.06	60.9	-7.82	76.53	50.3	26.2
4	48.97	59.5	-10.50	71.32	76.9	-5.56	93.67	81.3	12.4
5	66.51	76.5	- 9.96	87.75	84.9	2.87	108.98	88.3	20.7
6	69.04	71.5	- 2.43	89.16	87.9	1.28	109.28	103.3	6.0
7	77.57	81.5	- 3.90	96.57	92.9	3.69	115.57	95.3	20.3
8	99.83	95.5	4.36	117.71	110.9	6.8	135.59	122.3	13.3
9	118.13	101.5	16.66	134.9	126.9	8.02	151.66	142.3	9.4
10	115.62	98.5	17.15	131.26	124.9	6.38	146.91	147.3	-0.4
11	125.27	130.5	- 5.20	139.8	135.9	3.92	154.33	144.3	10.0
12	157.47	157.5	0	170.88	170.9	0	184.29	184.3	0
13	198.25	189.5	8.78	210.55	216.9	-6.33	222.84	238.3	-15.5
14	242.26	231.5	10.79	253.44	254.9	-1.44	264.61	275.3	-10.7
15	287.66	-59.5	-12.80	297.72	-59.1	-3.16	307.78	-50.7	- 1.5
16	-19.96	61.5	-81.42	-11.01	4.9	-15.89	-2.07	-15.7	13.6
17	182.63	166.5	16.16	190.45	188.9	1.57	198.28	215.3	-17.0
18	208.87	191.5	17.40	215.58	208.9	6.7	222.28	223.3	- 1.0
19	192.87	167.5	25.40	198.46	184.9	13.58	204.04	206.3	- 2.3
20	197.77	190.0	7.77	202.24	202.2	0	206.71	216.0	- 9.3
21	221.48	215.0	6.55	224.84	224.8	0	228.19	220.0	8.2
22	234.54	235.5	-0.93	236.78	230.9	5.9	239.01	227.3	11.7
23	229.55	217.5	12.08	230.67	226.9	3.79	231.78	228.3	3.5
24	239.54	230.5	9.07	239.54	233.9	5.66	239.54	226.3	13.3

sheets larger than 2 x 3 feet. In production, it may be possible to use other printed circuit material, such as thin copper epoxy-glass, at a minor increase in insertion loss.

The measured data on the breadboard dual column series feed show that the maximum measured VSWR was 1.16 into the lower beam input and 1.12 into the upper beam input over the band 1.2 to 1.4 GHz. The theoretical patterns for the upper and lower beams with ideal illumination functions are given in figure 3-7. The calculated patterns resulting from the measured illumination functions are given in figures 3-8 through 3-10.

Tables 3-1 and 3-2 summarize the amplitude data measured for the lower and upper beams, respectively. The network loss is obtained from the data by integrating the total power out of all 24 ports as shown in the tables. At center band, the loss is 1.3 dB for both beams (including 0.25 dB for 3 feet of 0.141 cable on the inputs). For the lower beam, the measured amplitude follows the theoretical to within 1.2 dB at center band, and to within 2.5 dB at the band edge.

The amplitude deviation from theoretical is systematic, with higher amplitude at the center and lower amplitude at the end of the array. This is an increase in edge taper and has minimal effect on the pattern. In a series feed, very small coupling changes in each coupler can accumulate across the feed to have larger effects on the edge taper but, generally, these edge taper effects are close to symmetrical and do not affect the patterns. This performance is adequate to meet the performance requirements as shown in the resulting antenna patterns of figures 3-8 through 3-10. The upper beam amplitude error is greater than the lower beam error, especially at the band edges. This is due to the fact that the upper beam illuminations are formed by more complicated multi-path vector additions. However, the elements with the greatest error are low amplitude and have small effect on the pattern. The antenna patterns of figures 3-8 through 3-10 show that this is adequate to meet the specifications.

The measured phases and phase errors for the lower and upper beams are summarized in tables 3-3 and 3-4, respectively. Again, the lower beam has the best performance; however, the resulting antenna patterns for both beams are adequate. The largest phase error, 81.42 degrees, occurs for the upper beam at the band edge at element 16. For the upper beam, the illumination amplitude at this element is close to a null (greater then 30 dB down) and has practically no effect on the antenna pattern. The output voltage at this element is the sum of two component vectors, one from the primary line and one from the secondary, which are very close in amplitude and about 180 degrees apart in phase, and add to form a null. For this case, small phase errors in either component are greatly magnified in the resulting null.

In conclusion, the network meets the specification requirements of forming simultaneous lower pencil beam and upper csc^2 beams with 15 dB maximum sidelobes over a broadband (1.2 to 1.4 GHz) with low loss.

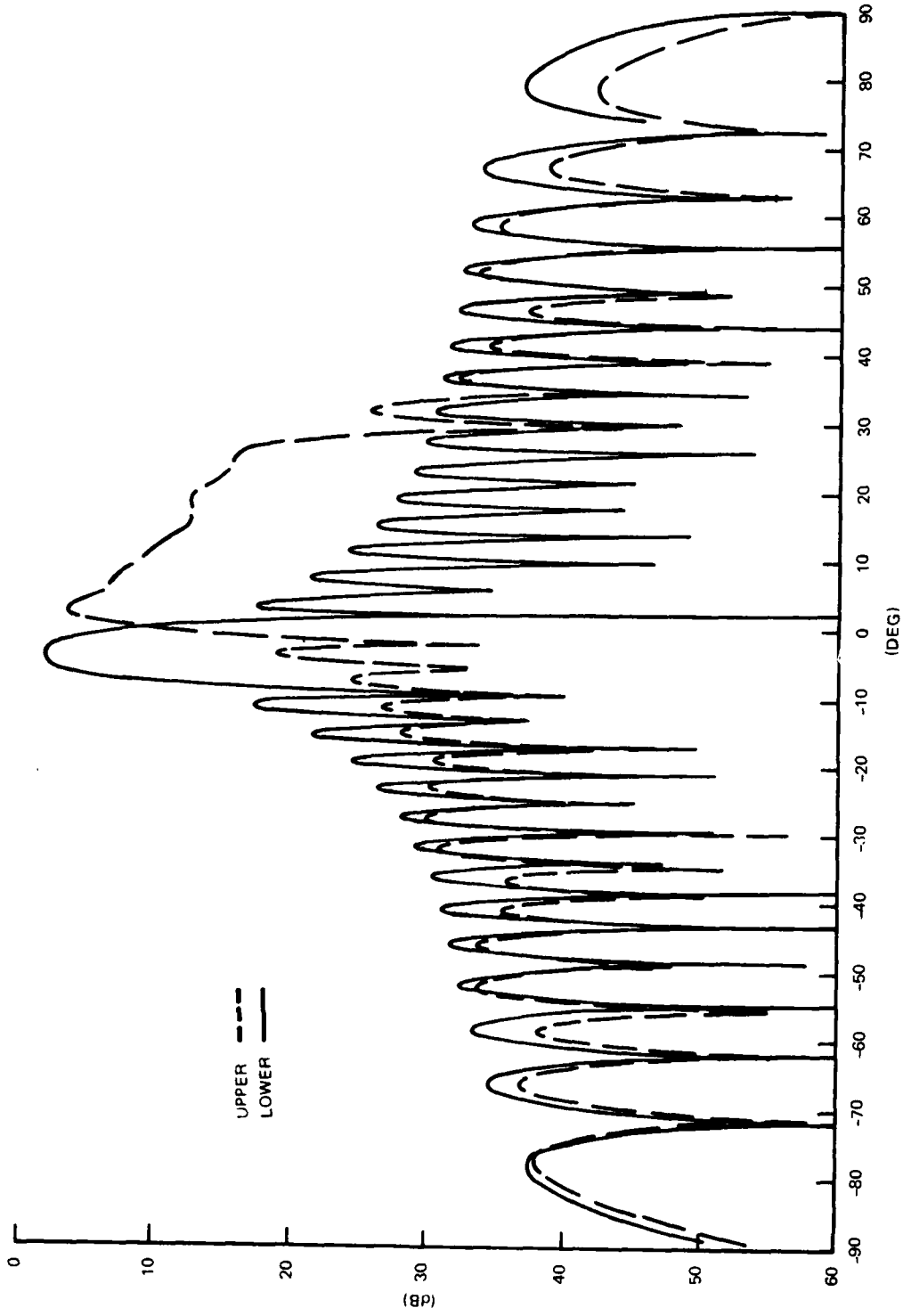

Figure 3-7. Theoretical Patterns for Upper and Lower Beams - 1.3GHz

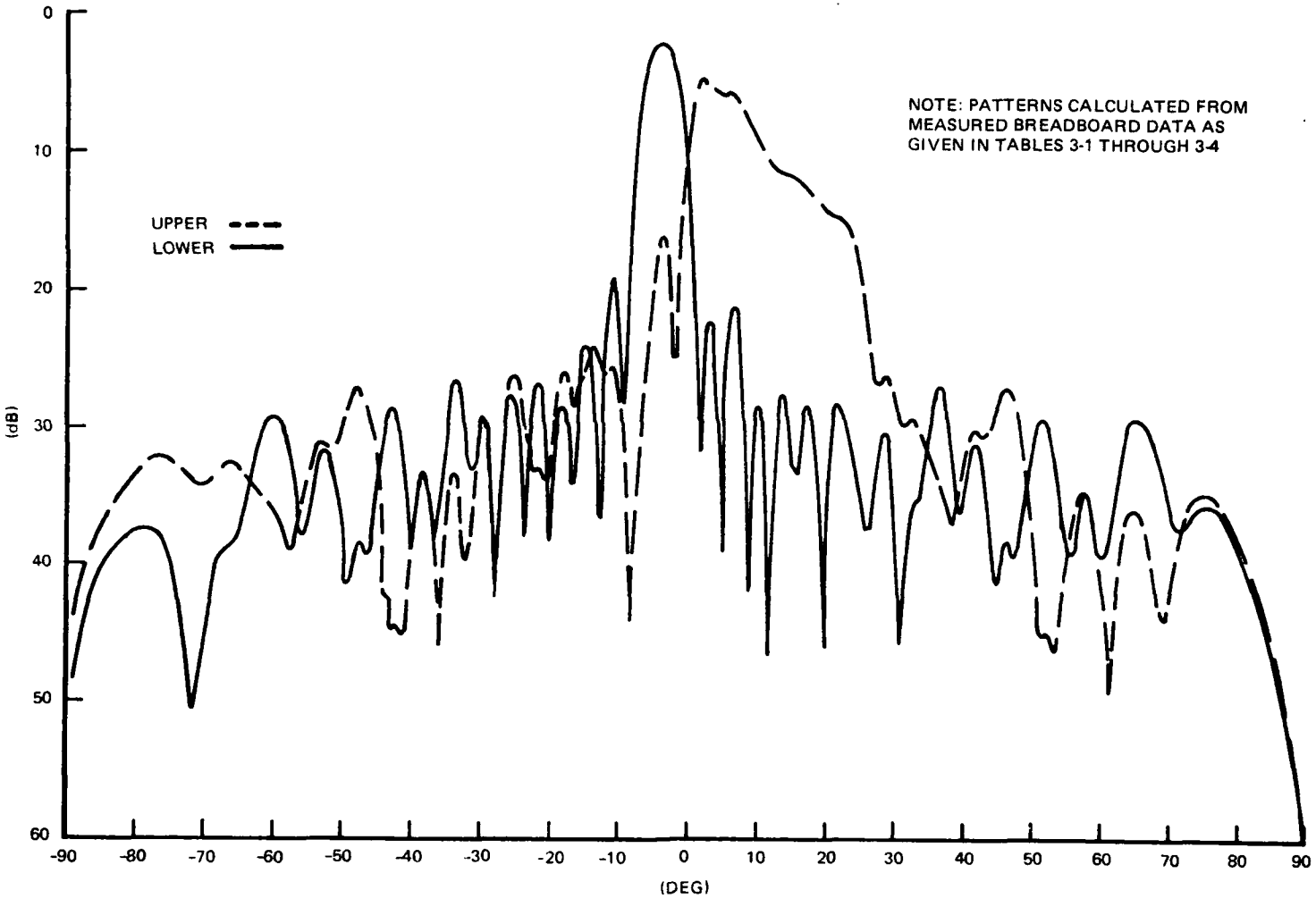

Figure 3-10. Calculated Patterns for Upper and Lower Beams - 1.4GHz

Section 4

STRIPLINE FABRICATION TECHNIQUES

4.1 TASK SUMMARY

The objectives of this task were to investigate fabrication techniques for the stripline column network with emphasis on electrical performance, ease of manufacturing, cost, structural integrity, and light weight.

4.2 STRIPLINE CONFIGURATIONS

Three basic configurations were considered and compared for use in the final unattended radar production column networks. The configurations are shown in cross section in figures 4-1, 4-2, and 4-3. The first configuration, figure 4-1, consists of the etched stripline circuit sandwiched between low dielectric constant sheets which are in turn sandwiched between 1/8-inch thick aluminum ground planes. Ground plane spacing is maintained by 1/4-inch thick by 5/8-inch diameter round metal spacers distributed periodically throughout the network. This configuration works well electrically, and it is ideal for breadboarding since the stripline is not permanently captivated between the ground plane, and the network can easily be opened for changes. The dielectric can be spongy foam such as Emerson & Cummings PP or it can be rigid polyurethane since the 1/4-inch thick by 5/8-inch diameter metal spacers provide the ground plane spacing. Loss measurements shown in figure 4-4 have been made on samples built in this configuration. The disadvantages of this configuration is its weight of 3.6 pounds per square foot (which results in a weight of 130 pounds for a 3- by 12-foot column network) and insufficient structural rigidity of a 12-foot long panel. This configuration sags of its own weight over a 12-foot span.

To reduce the weight and increase the structural rigidity of the panel, the configuration of figure 4-2 was developed. Here, the outer ground planes are each in themseleves a sandwich consisting of a thin 0.040-inch aluminum sheet and an even thinner 0.010-inch aluminum sheet sandwiching a 1/2-inch thich, 2 pound per cubic foot density structural polyurethane sheet. These outer panel are assembled on a flat table using epoxy glue to cement the layers. Although the outer panels are made of very thin aluminum, they are extremely rigid due to the increased section modulus provided by the 1/2-inch thick structural polyurethane. The outer panels replace the 1/8-inch thick aluminum sheet of figure 4-1, resulting in a lighter, stiffer configuration which still retains the advantage of being able to open and remove the inner printed circuit for breadboarding and changes since only the outer panels are glued.

This construction, figure 4-2, has also been used to build 30 networks, each of which is 12 by 2.5 feet, for a similar program. The construction technique results in an extremely rigid board which can be used as a structural support member to support other components and the array face, as well as being self-supporting. Use of this technique could eliminate

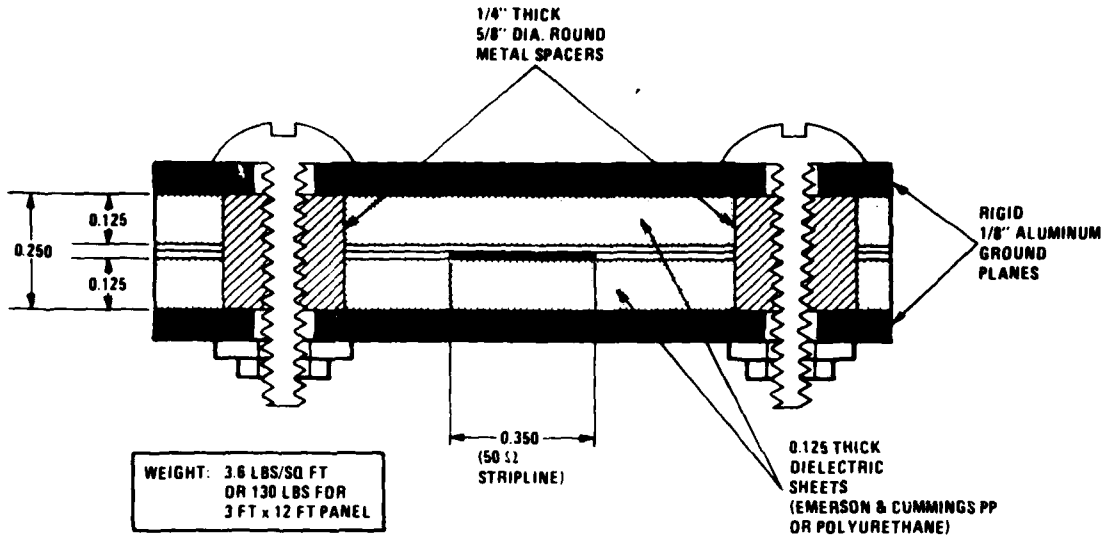

Figure 4-1. Stripline-Configuration 1

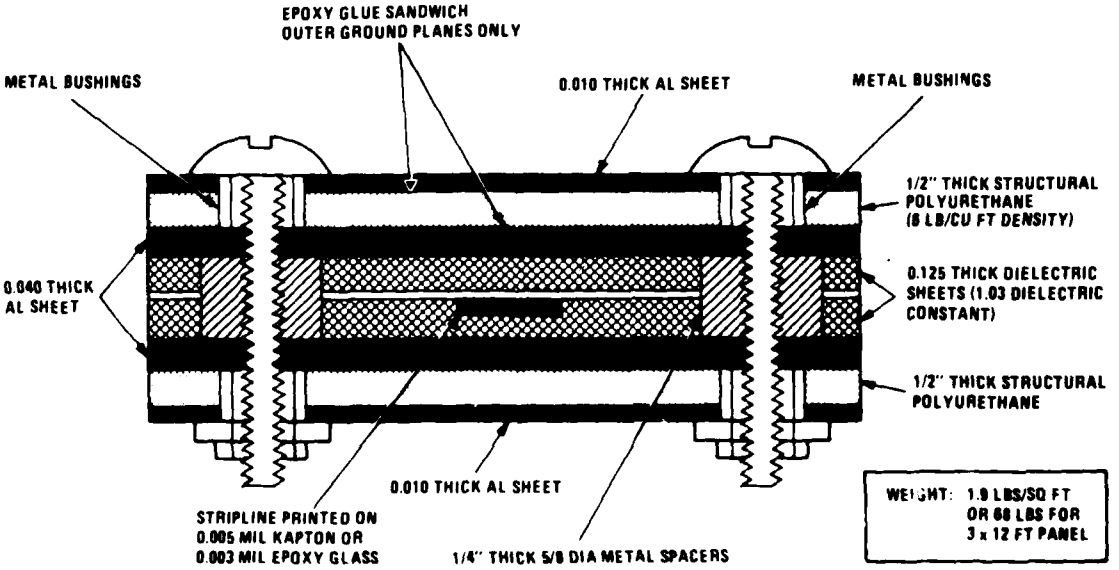

Figure 4-2. Stripline-Configuration 2

the need for external structural members. The weight of a 3- x 12-foot panel would be 61 pounds when built in this manner, which is one-half the weight of the original configuration of figure 4-1.

A third technique which has been studied is shown in figure 4-3. This technique would result in an extremely light weight column network, a 12- by 3-foot panel being only about 7 pounds. The unit consists of a stripline sandwiched between dielectric layers of polyurethane or HEXCEL which are in turn sandwiched between layers of 0.006-inch thick aluminum sheet. The layers are glued together using 4 layers of Surlyn adhesive sheets which are heat cured in a press in a large oven. Two 12-foot experimental sections were built with this technique. One section contained polyurethane (Trymer) foam dielectric and the second section contained HEXCEL dielectric. On each section, half of the stripline circuitry was printed on 0.003-inch thick Kapton, and half was printed on 0.005-inch thick epoxy fiberglass so that the various combinations could be evaluated electrically and mechanically. Loss and phase measurements were made on these sections and are summarized in figure 4-4. The various combinations are listed in the figure in order of increasing loss. The effective dielectric constant and wavelength are also listed. The wavelength varies by 3 percent for all of the combinations. The broadband dual column network which can operate over a 15 percent bandwidth could therefore be printed and built in any of these combinations.

Mechanically, the laminated sections were very light weight. However, they were more fragile than cicuits built in the technique shown in figure 4-2. These laminated sections would require external support structures in a system, whereas that described in figure 4-2 is self-supporting.

As described in an interim report, an earlier 12-foot laminated section exhibited loss resonances at several frequencies over the band. This problem was cured in the final two laminated sections by improving the flatness of the panels. The final panels were heat cured on a flat platen.

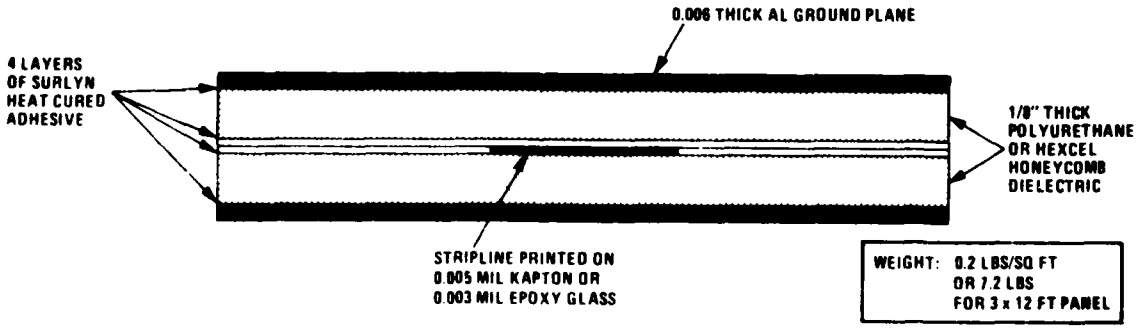

Figure 4-3. Stripline-Configuration 3

MATERIAL	MEASURED LOSS AT 1.385 GHz	MEASURED λ_g AND EFFϵ_r AT 1.385 GHz
EMERSON & CUMMINGS PP FOAM (ϵ_r = 1.03) + KAPTON PC (0.003 THICK)	0.0045 dB/IN 0.054 dB/FT	λ_g = 8.2284 IN EFFϵ_r = 1.074
EMERSON & CUMMINGS PP FOAM + EPOXY FIBERGLASS PC (0.005 THICK)	0.007 dB/IN 0.084 dB/FT	λ_g = 8.1346 IN EFFϵ_r = 1.099
UPJOHN TRYMER CPR 9545 POLYURETHANE + KAPTON PC (0.003 THICK)	0.008 dB/IN 0.096 dB/FT	λ_g = 8.1090 IN EFFϵ_r = 1.106
UPJOHN TRYMER CPR 9545 POLYURETHANE + EPOXY FIBERGLASS PC (0.005 THICK)	0.01 dB/IN 0.12 dB/FT	λ_g = 8.0295 IN EFFϵ_r = 1.128
HEXCEL HRH-10 3/8 CELL SIZE + KAPTON PC (0.003 THICK)	0.011 dB/IN 0.132 dB/FT	λ_g = 8.0510 IN EFFϵ_r = 1.122
HEXCEL HRH-10 3/8 CELL SIZE + EPOXY FIBERGLASS PC (0.005 THICK)	0.013 dB/IN 0.156 dB/FT	λ_g = 7.970 IN EFFϵ_r = 1.145

Figure 4-4. Loss Measurements

4.3 FABRICATION AND INSTALLATION TECHNIQUES

The following is a detailed description of the fabrication techniques for two different column network panel designs, together with a production cost comparison of the two designs. The first structural design is similar to figure 4-2; the second, a thermally pressed laminated design, is similar to figure 4-3. Both designs may be packaged, with variation in detail, for adaptation into a complete column network array. The stripline circuit used in the two designs is the same, except for the requirement of clearance holes in the substrate in some cases.

Figures 4-5 and 4-6 show the basic design, in cross section, of the two types of network assemblies. Figures 4-7 and 4-8 are assembly drawings which demonstrate the use of these designs in an antenna array.

The design shown in figure 4-5 and in detail in figure 4-7 is a structural panel sandwich assembly which consists of two pre-assembled structural panels bolted together to make up a sandwich assembly.

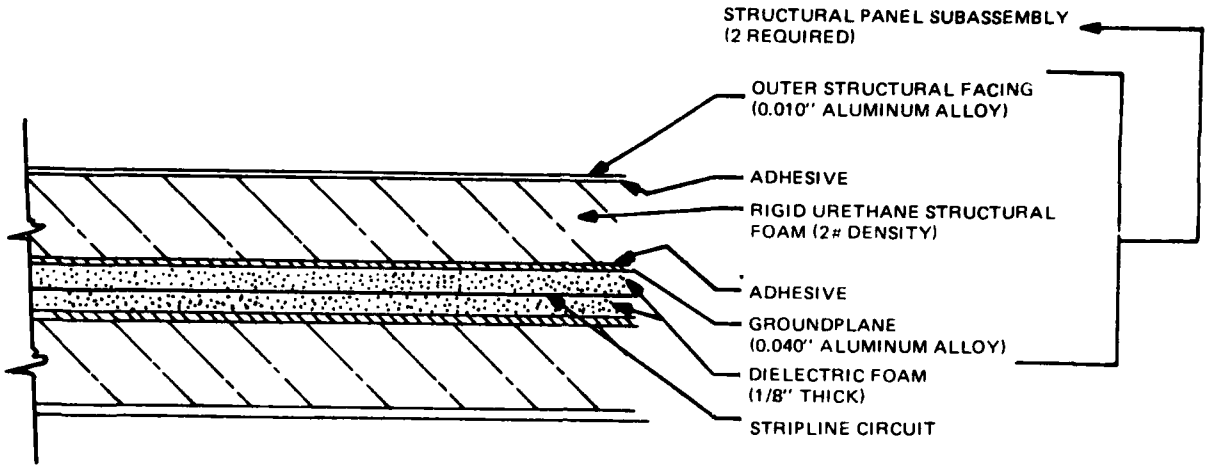

Figure 4-5. Structural Panel Network Assembly

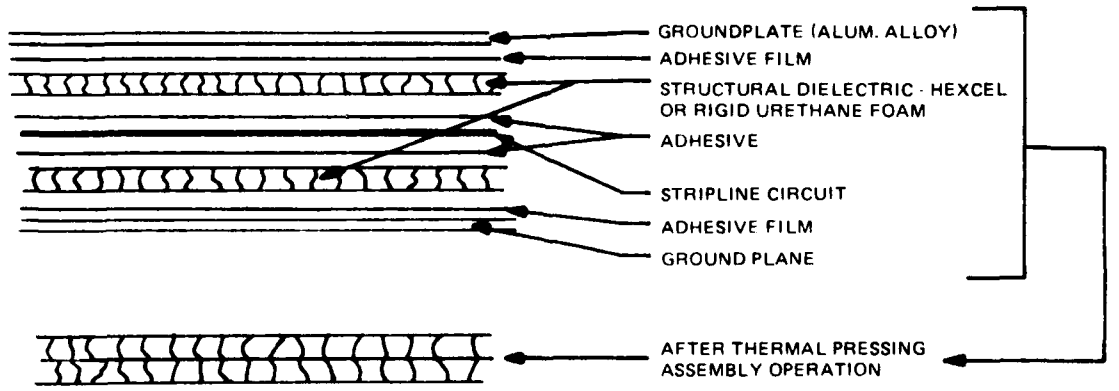

Figure 4-6. Press Laminated Network Assembly

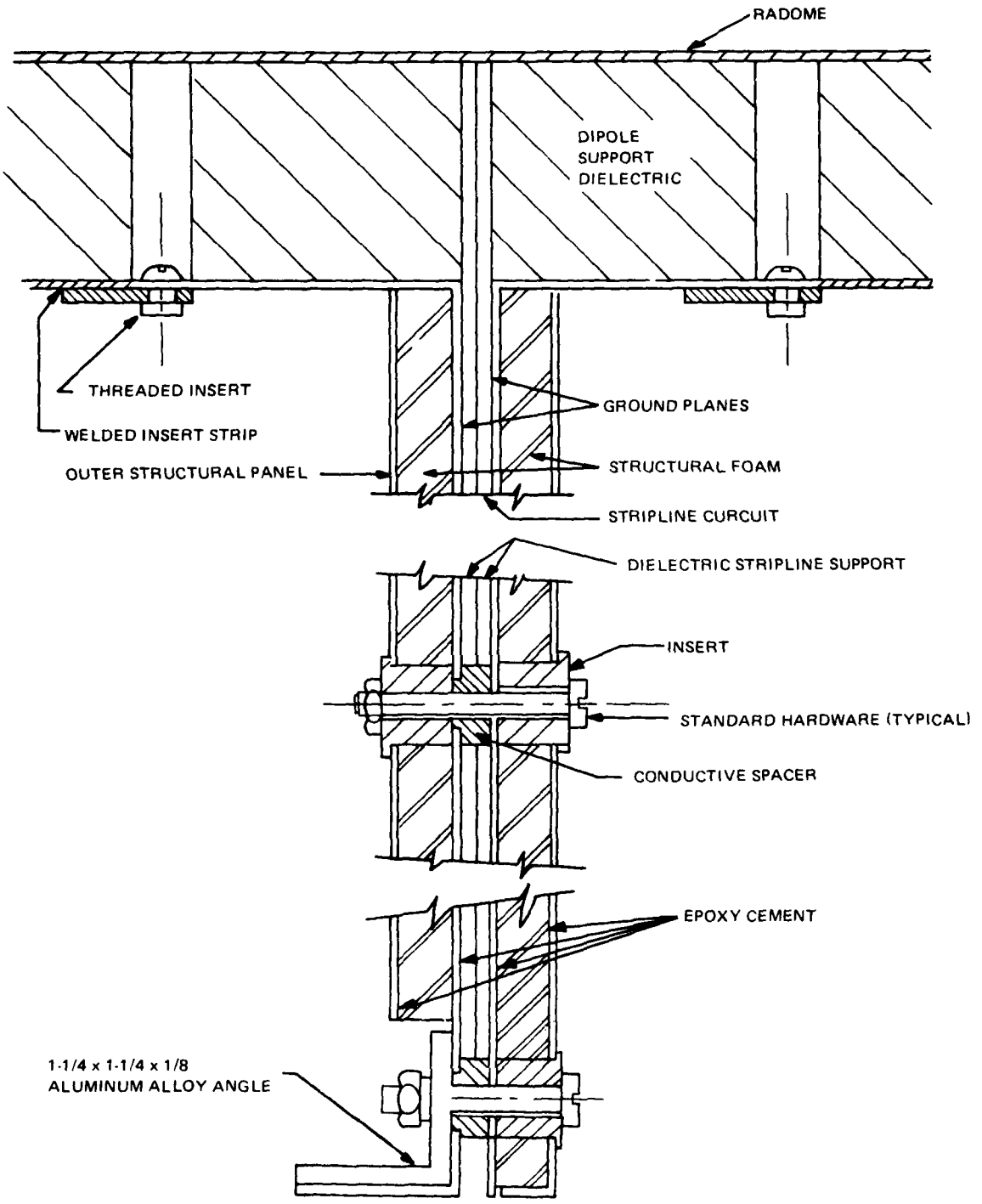

Figure 4-7. Column Network Assembly (Structural Panel)

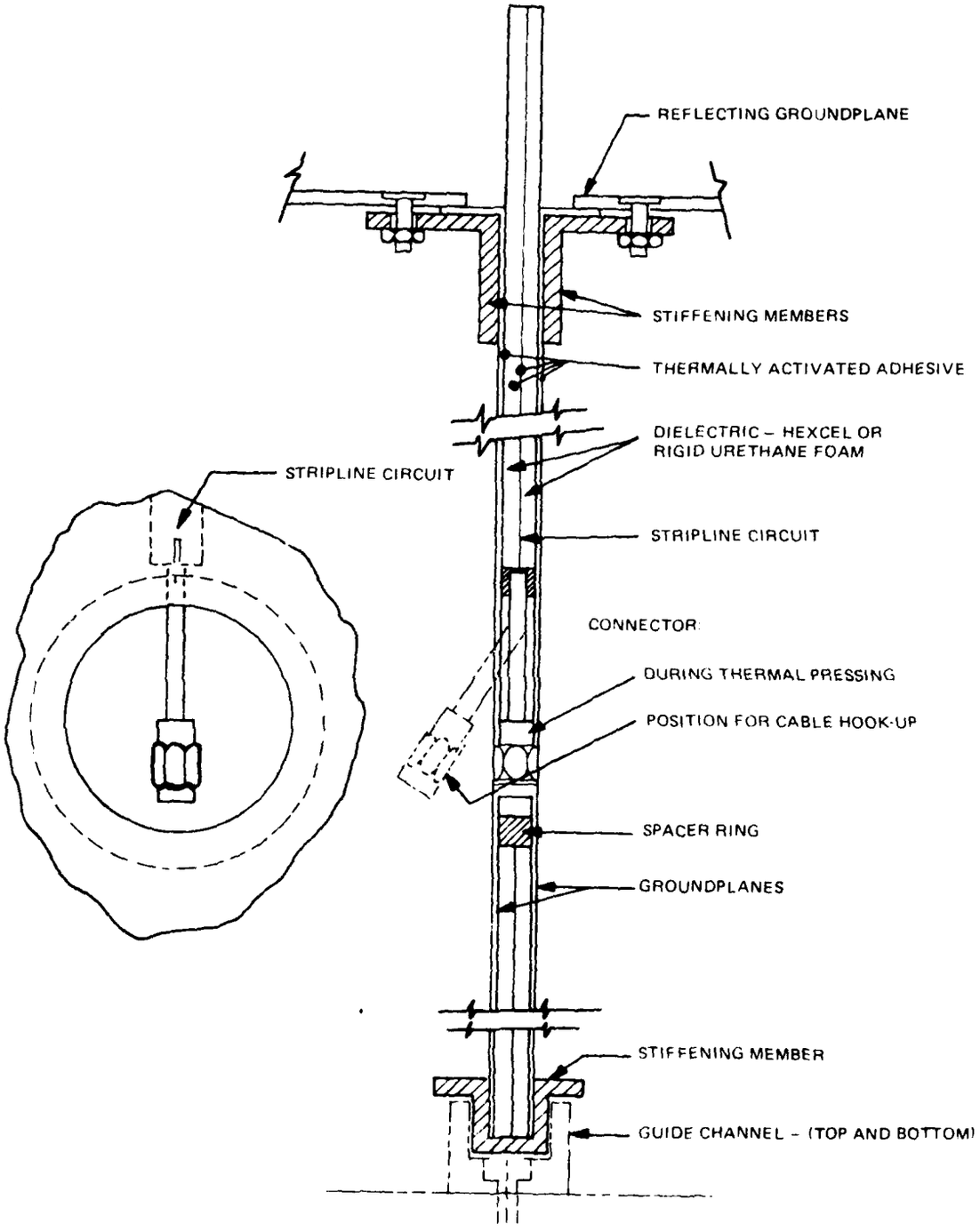

Figure 4-8. Column Network Assembly (Press Laminated)

Each subassembly panel comprises the metal face materials, with bolt holes and ground plane bends formed, cemented to the rigid urethane structural foam core. The panel is cemented so that metal face material that serves as the ground plane is flat to within 0.003 inch over any 24 inches length of panel; this requirement is necessary for efficient microwave performance. The flatness is achieved by curing the panels on a flat jig plate if cemented, or using platens of proper flatness if cemented by means of a thermal press operation. After the cementing operation, the bolt holes are redrilled to remove the core material in order to insert the metal bushings of the assembly hardware.

The bolt hole pattern is also cut in the dielectric foam stripline circuit support to provide clearance for the ground plane separating spacers. The two layers of dielectric foam locate the stripline circuit at the midpoint between the ground plane surfaces.

Figure 4-7 shows (at the top of the illustration) a section of a structural panel assembly joined at the reflective ground plane, below that, a typical spacer insert and screw assembly, and finally, the adaptation of a structural angle into the assembly for installation into an antenna array.

This type of column network assembly can be used as a structural element of an antenna package. However, its greater weight and cost of assembly must be considered when compared to those of the alternate design.

The press laminated network assembly is shown as a basic design in figure 4-6 and as a detailed assembly in an array in figure 4-8. This assembly is made up as a laminate with the dielectric material on each side of the stripline circuit functioning as the structural core which holds the two metal ground planes together in a cemented assembly. The dielectric material maintains the 0.003-inch flatness and parallelism of the aluminum ground planes of this laminated assembly.

This panel is best assembled in a thermal press, several at a time, using a thermally activated adhesive film (Surlyn 1632) or a resin, impregnated into a 0.003-inch thick glass cloth carrier.

In the interest of minimizing the weight of an assembly because of the many panel assemblies used in an array, the facing or ground plane aluminum alloy is only 0.010-inch thick. A laminated assembly with 0.010-thick aluminum facing and 0.25-inch, 2-pound density core is not extremely rigid with respect to its 144-inch length. Analysis indicates a 4.1-inch deflection (when laid flat rather than on edge) over the 144-inch length, due only to the panel's own weight. To permit handling and shipping, stiffening elements must be epoxy and/or screw fastened to the panel after the thermal pressing operation. The stiffeners give the panel the required rigidity for handling and also serve to facilitate assembly into guide slots or channels of an antenna array assembly.

Figure 4-8 shows a section through a laminated panel assembly. The stiffening elements at the ground plane also serve to hold the ground

plane surfaces in contact with the reflective ground plane of the array structure.

4.4 PANEL FABRICATION FOR PRESS LAMINATE METHOD

The two panels assembled by the press laminate method for electrical test were made using two different dielectric/structure core materials; these materials were rigid urethane foam of 2-pound density and a HEXCEL aramid fiber/phenolic resin honeycomb. The press laminate method is described on page 49, and a cross section is shown in figure 4-3. A more detailed view is shown in figure 4-8.

Table 4-1 shows a comparison of these two materials with respect to the physical characteristics pertinent to their use in the column network assemblies.

Examination of the physical characteristics of the two dielectric/core materials used for test assemblies of the column network indicates that the honeycomb (HEXCEL) material is the better of the two materials for this application. The honeycomb material not only is better from the standpoint of strength, temperature range, water absorption, and availability, but it also is more easily handled in laying-up the laminate. The 1/8-inch thick urethane foam is quite fragile and requires cleaning to remove fine particles of foam which are a residue from the machining (sawing) of the buns of foam.

Table 4-1. Comparison of Physical Characteristics

Parameter	HEXCEL HRH 10, 2-pound Density Honeycomb, 3/8-in Cell, 1/8-in Thick	Urethane Foam, 2-pound Density, 1/8-in Thick
Compressive Strength (psi)	170 typ, 106 min	38 typ, 22 min
Shear Strength (psi)	L-axis - 110 typ, 22 min W-axis - 55 typ, 36 min	35 typ, 18 min
Temperature Range (^{o}F)	-100 to 450	-320 to 300
Loss of Compressive Strength at 250^{o}F - Thermal Pressing Strength	10%	40%
Source of Supply	HEXCEL Corp. 96 x 44-inch sheets; larger sizes available in quantity	Upjohn CPR Division 4 x 1 x 1-foot buns - cut to size (approximately 45 x 10 x 1/8 inch)
Adaptability	Easily handled, flexible, ready for assembly	Fragile, requires light brushing to remove residue from sawing. Easily fractured in handling.
Cost	$0.65/sq ft (8/79)	$0.40/sq ft for materials, plus machining - estimate $0.60/sq ft

4.5 MANUFACTURING COST COMPARISON

The cost of producing large quantities of networks of each design described in subsection 4.3 is summarized in table 4-2. The cost breakdown is based on experience at Sperry in manufacturing 30 structural panel type column network assemblies, figure 4-5, several prototype assemblies of the thermally pressed laminate assemblies, figure 4-6. and from vendor data for lamirated assemblies.

Table 4-2. Cost Summary

Item	Structural Panel Assembly ($)	Press Laminate Assembly ($)
Circuitry		
Circuit board material	50	50
Circuit processing	75	75
Circuit component assembly	15	15
Circuit splicing	10	10
Sheet Metal		
4 with 75-hole pattern	240	—
2 with 2-hold pattern	—	45
Stiffener Elements	—	10
Angle Section	12	—
Structural Frame	76	—
Dielectric	20 (foam)	30 (HEXCEL)
Spacer	12	—
Hardware	12	—
Adhesive	negligible	negligible
Labor		
Lay-up laminate and thermal press time	—	62
Cement structural panel	15	—
Redrill clearance holes	12	—
Mechanical assembly of 1/2 panel	10	—
Mechanical assembly of full panel	20	—
	$579	$297

4.6 INSTALLATION REQUIREMENTS

Support structures will be required for installation of the column network assemblies into an array.

The structural panel design was installed by fastening the structural angle section to a support member of the antenna package. The ground planes were then fastened together by means of a ground plane strip between

each assembly as shown in figure 4-7. The structural angle at the top and bottom edge were used to attach the sheet metal housing element of the antenna package. Spaced at 5.140 inches, these assemblies result in an extremely stiff structural package, weighing approximately 61 pounds for a 3 by 12-foot board.

In contrast, the press laminate network assemblies, figure 4-8, are less than 9 pounds per 3x12-foot board. However, these boards are not self-supporting and require additional structure to take up the effects of wind loads. The added structure consists of ground plane supports and guides for inserting the laminated panels into the array. This structure weighs approximately 30 pounds per board, resulting in a total of 39 pounds per board.

Section 5

DEVELOPMENT OF STRIPLINE COMPONENTS

5.1 TASK SUMMARY

The object of this task was to develop the stripline components required to make the dual beam column network which is described in section 3. The components are 2- and 3-branch directional couplers, crossovers, terminations, and the radiating dipole. The component development is complete, as is the network layout incorporating these components (see figure 3-1).

5.2 BASIC STRIPLINE

The dual channel column network is constructed in a symmetrical stripline configuration which consists of transmission lines etched on 0.003-inch thick Kapton sheets with 0.0014-inch thick copper cladding on one side. The ground plane spacing is 0.250-inch, and is determined by sandwiching the circuit between two 0.125-inch thick polyurethane foam spacer sheets. Thin aluminum sheets form the outer ground planes.

The curves of figure 5-1 were derived from information gathered in past experience on programs which dealt with networks constructed in symmetric stripline supported by materials other than air. These curves depict the phase velocity (V_P), as a function of the strip width to ground plane separation ratio (w/b), for Kapton surrounded by polyurethane foam and for epoxy/fiberglass material surrounded by HEXCEL HRH 10. Figures 5-2 and 5-3 show the characteristic impedance versus w/b for each construction technique.

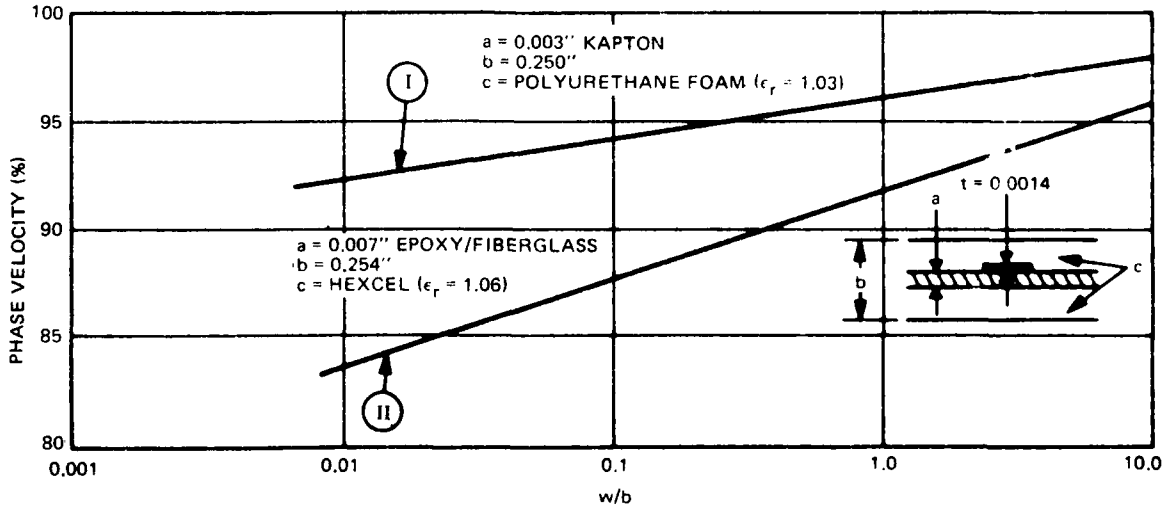

Figure 5-1. Phase Velocity Versus w/b (Referenced To Air)

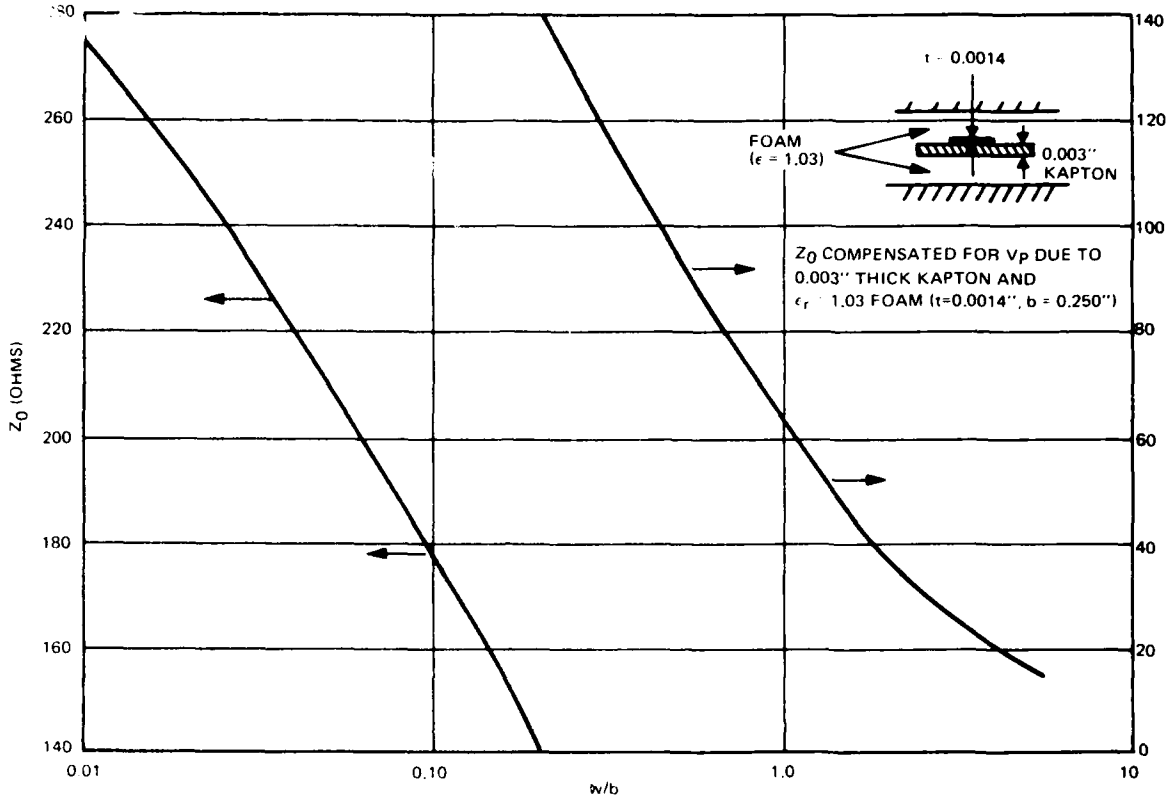

Figure 5-2. Z_o Versus w/b (Kapton)

5.3 COUPLER DEVELOPMENT

The series feed network requires a total of 43 different coupler designs whose coupling values range from 3.41 dB (C_{max} = 0.6755) to 12.03 dB (C_{min} = 0.2502). The coupler requirements were very influential in determining the feed circuit stripline configuration.

Quarter-wave edge and broadside parallel-coupled structures were considered for this application, but were rejected for the following reasons. The edge-coupled configuration is useful for loose coupling, but is very rarely used for couplers which are tighter than 6 to 8 dB; conversely, the broadside structure is principally used for very tight coupling and is not good for couplers looser than about 6 to 8 dB. Neither coupler is adequate to cover the full range of coupling values required in this network. Additionally, the broadside type requires a three-layer asymmetrical stripline configuration which has inherent registration problems, especially for a circuit of this size and complexity. It would result in a costly package.

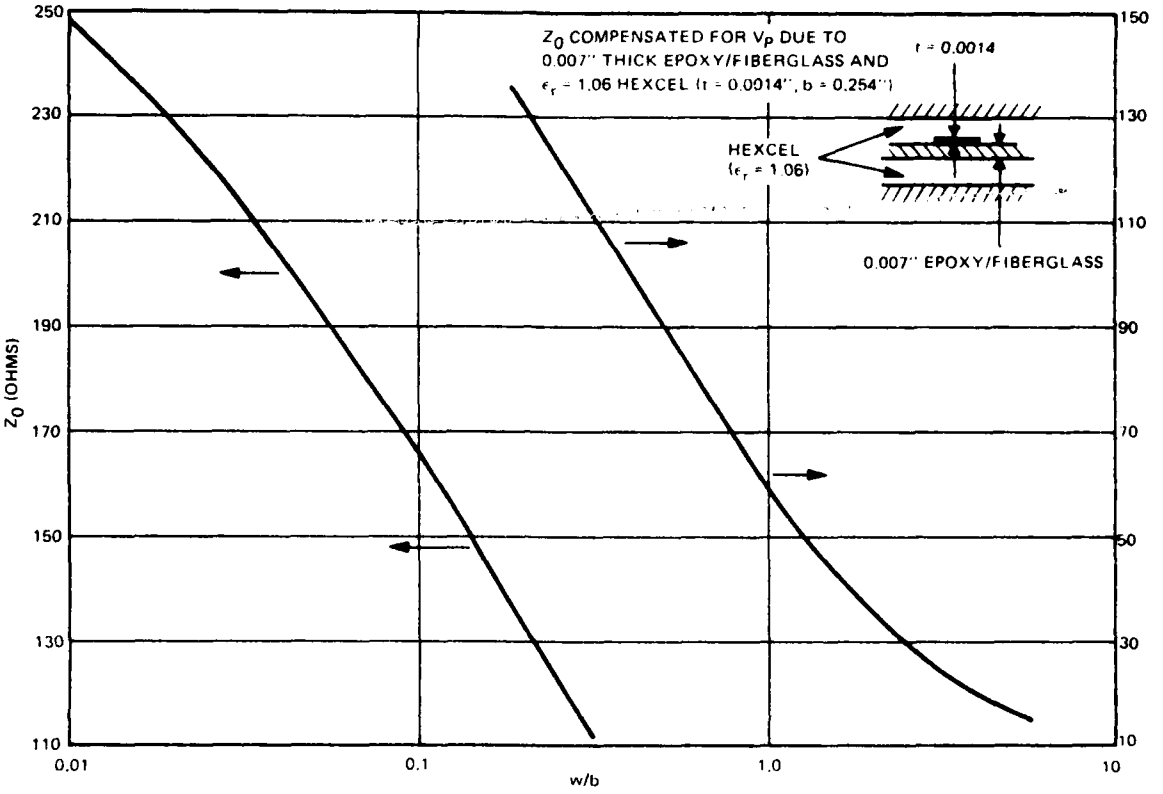

Figure 5-3. Z_0 Versus w/b (Epoxy/Fiberglass)

Therefore, branch guide directional couplers were chosen because they can be printed on one side of the stripline sheet and because they are capable of covering the range of coupling values required. Two- and three-branch designs are utilized.

Three-branch couplers are desired throughout the network because of their excellent bandwidth characteristics. However, there is a physical limitation present which governs the use of this type coupler in stripline. It is impractical to print and etch stripline RF lines which are less than 0.010-inch wide and expect a high probability of no defects in the finished product; therefore, it was decided to limit the narrowest line to 0.013-inch. The loosest required three-branch coupler than can be built using this guideline has a coupling value of 6.73 dB. Therefore, couplers ranging from 3.41 dB to 6.73 dB are three-branch, and those from 6.73 db to 12.03 dB are two-branch.

As seen from the results of a computer analysis, figure 5-4, both type couplers are adequate for this network, displaying very satisfactory VSWR, minimum isolation, and coupling variation characteristics over the band width of interest.

Because it was not cost-effective to design, build, and test every coupler of the large number required, it was decided to follow the procedure in which five 3-branch couplers, whose coupling values spanned the required range, were selected to be built and tested. Based on those test results, a set of curves was developed which fully describes each physical dimension of any coupler in the range. These curves are shown in figure 5-5. It was determined from computer analysis that optimum results could be achieved by using only two different impedances for the series branches (i.e., 45 ohms for coupling coefficients 0.4 through 0.52, and 40 ohms for C = 0.521 through 0.7). The center shunt arm impedance is dependent on the series arm impedance, thus the reason for two curves to find the width of the center arm. The outer shunt arm impedance depends only on the coupling coefficient and therefore only one curve is necessary. As an example of usage of figure 5-5, if coupling coefficient = 0.50, then A = 0.388, B = 0.020, C = 0.165 inch.

Numerous two-branch couplers were built and tested for a previous L-band column network program at a center frequency slightly higher than that required for this network. Measurements over a bandwidth equal to the unattended radar (15%) bandwidth verified the computer results shown in figure 5-4. It was therefore decided to scale the center frequency of these designs when two-branch couplers were required.

THREE-BRANCH COUPLER

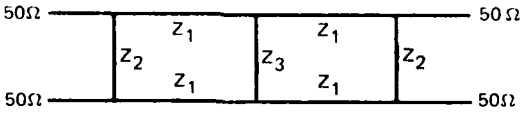

COUPLING	Z_1	Z_2	Z_3	VSWR (BANDEDGES)	MINIMUM ISOLATION	COUPLING VARIATION
3.41dB	40Ω	128.6Ω	47.4Ω	1.048	32.4dB	± 0.058 dB
6.73dB	45Ω	204.9Ω	87.9Ω	1.012	38.5dB	± 0.45dB

TWO-BRANCH COUPLER

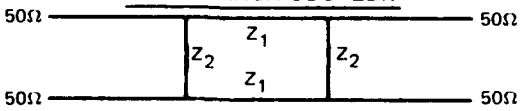

COUPLING	Z_1	Z_2	VSWR (BANDEDGES)	MINIMUM ISOLATION	COUPLING VARIATION
6.73dB	44.38Ω	96.35Ω	1.08	22.2dB	± 0.048dB
12.03dB	48.4Ω	192.7Ω	1.022	28.4dB	± 0.046dB

Figure 5-4. Summary of Results of AMCAP Analysis of Branchline Couplers

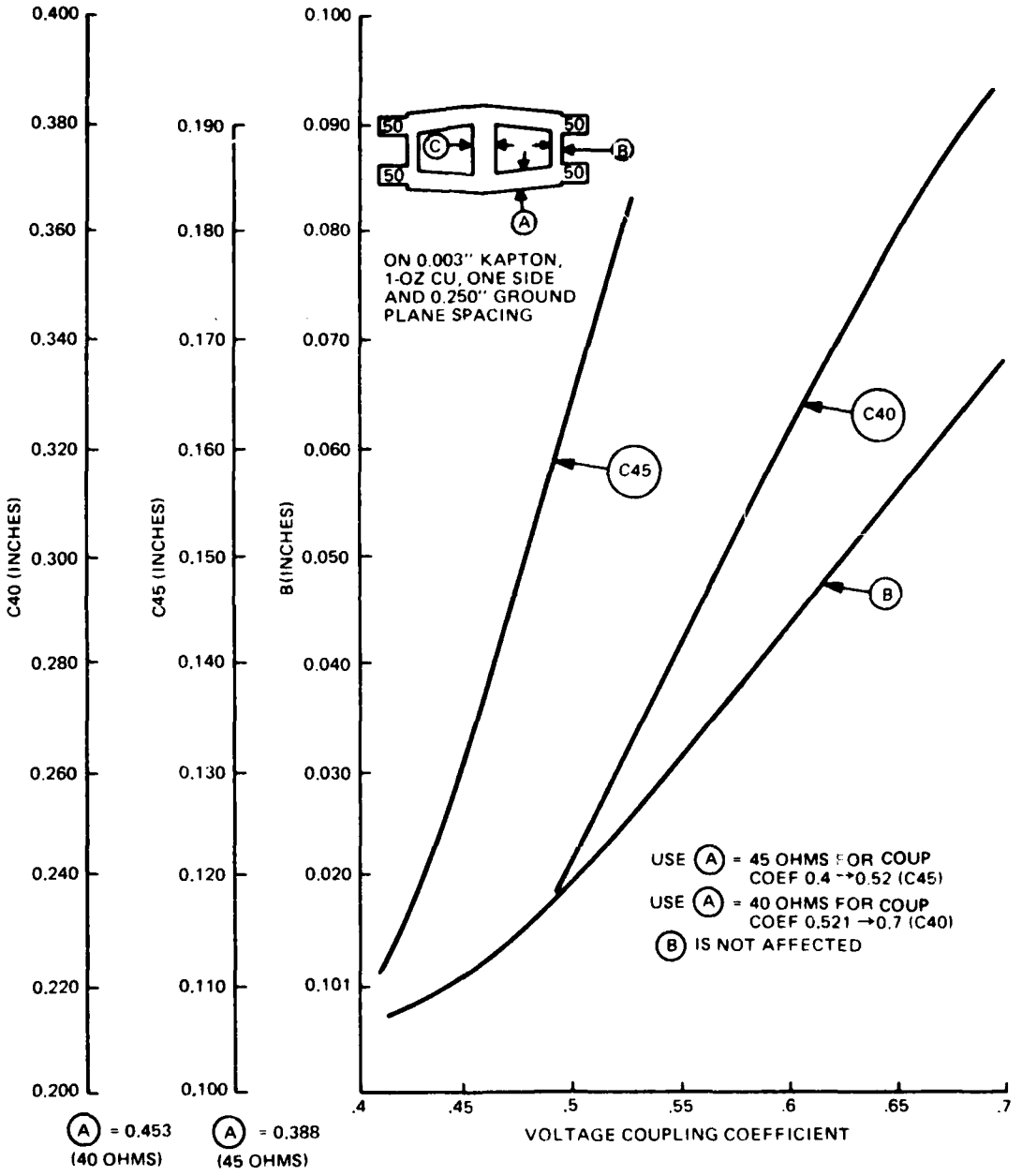

Figure 5-5. Line Widths Versus Coupling Coefficients - Three-Branch Coupler Design

Table 5-1 describes the data taken on the five 3-branch selected couplers. The measured coupling was within 0.1 dB of theoretical, except for the 6.96 dB coupler, which measured within 0.25 dB. Isolation, VSWR, and coupling variation over the bandwidth were all within acceptable limits.

Table 5-1. Data on Five 3-Branch Directional Couplers and Comparison of Measured Results to Theoretical

Theoretical Coupling	Measured Coupling	Maximum VSWR		Minimum Isolation		Coupling Variation	
		Theor.	Meas.*	Theor.	Meas.	Theor.	Meas.
3.41 dB	3.3 dB	1.05	1.04	32.4 dB	24 dB	±.05 dB	±.07 dB
4.61 dB	4.6 dB	1.03	1.11	34.6 dB	28 dB	±.047 dB	±.05 dB
5.9 dB	5.8 dB	1.02	1.09	36.8 dB	28 dB	±.05 dB	±.06 dB
6.96 dB	6.7 dB	1.01	1.12	38.6 dB	28 dB	±.045 dB	±.10 dB
7.6 dB	7.5 dB	1.01	1.12	39.4 dB	26 dB	±.045 dB	±.025 dB

*Maximum VSWR including connectors and terminations.

At the point in time during the development program that these data had been gathered, it was determined from a design layout of the full network that the packaging problems could be significantly lessened if the 3-branch couplers could be made shorter in length. This necessitated development of a folded 3-branch coupler which required bends in series arms of the coupler. The dimensions of the five straight couplers described previously were altered in the following manner: Widths of shunt arms remained the same, whereas the length of the shunt arms were made equal to the algebraic average of the two different original lengths to simplify the design. The length and width of the series arms were modified to reflect the needed higher impedance and the change in phase velocity through the bends. Figure 5-6 shows a comparison of size of the straight and folded three-branch couplers for the 3.3 dB coupling value. Data taken on these folded couplers very nearly matched the data of the straight-arm coupler de-sign. Coupling data were within 0.1 dB of previously measured data. VSWR was as good or better, isolation improved on the average, and coupling variation remained the same (it improved to +0.05 dB for the 6.8 dB coupler). Figure 5-7 is typical

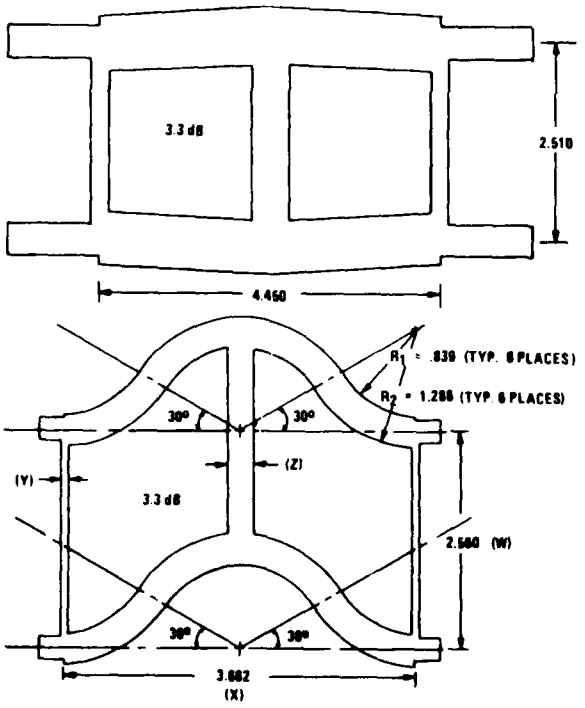

Figure 5-6. Comparison of Size of Straight and Folded Three-Branch Coupler Design

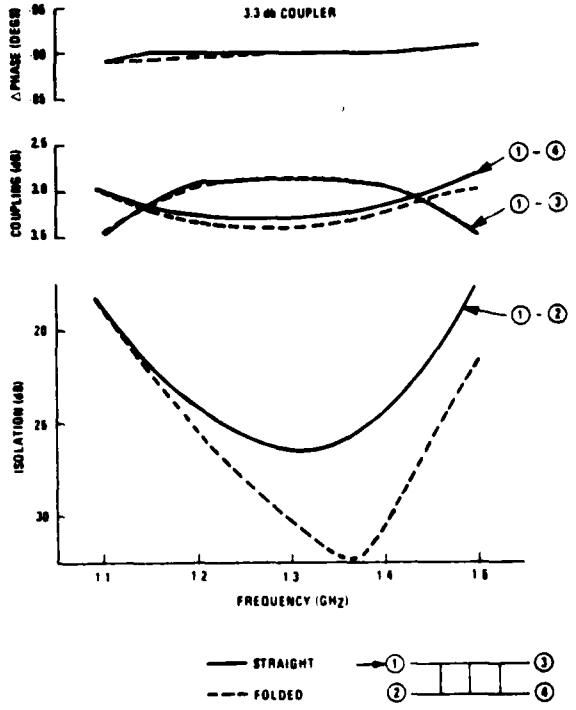

Figure 5-7. Typical Data Results Straight and Folded Three-Branch Coupler

of the data obtained on the three-branch straight and folded couplers.

The three couplers used in the central interlace area of the network are straight three-branch couplers because there is room there for this configuration (see figure 3-1).

Because of the possible weight advantage using HEXCEL in construction of a column netowrk, measurements were taken using HEXCEL HRH 10 as a spacer for a 6.7 dB folded three-branch coupler. The resultant data were no different than that obtained using polyurethane foam spacers and were not dependent on the spacer cell alignment (parallel or perpendicular to the RF line). Therefore, although the first dual column network was built using Emerson and Cummings PP dielectric, it will be possible to substitute any other dielectric such as HEXCEL or TRYMER in the final configuration so long as it has a low dielectric constant. The network itself is designed with "real time" line lengths and therefore should not be affected by small changes in dielectric constant.

5.4 TERMINATIONS

Terminations for all couplers were designed, built, and tested. They consist of a 51-ohm, 1/4-watt, carbon resistor, soldered in series with the 50-ohm RF line, terminated by an open-circuit length of 50-ohm line. This open-circuit length of line ($< \lambda/4$) matches out the inductive reactance of the resistor. VSWR is less than 1.15:1 over the bandwidth.

5.5 CROSSOVERS

The crossovers included in the layout of figure 3-1 consist of printed arrows with crossed 0.020-inch diameter wires soldered between the tips of the arrows. This design is inexpensive and lends itself well to any of the stripline construction techniques as described in Section 4. The 0.020-inch wires are inductive and are matched by the arrows which are capacitive, forming a low pass filter. This design has a VSWR which rises to a high of 1.2 at the upper end of the operating band (1.4 GHz). In addition, its isolation is

limited to 25 to 30 dB. The isolation was tolerable in the network design, and the VSWR is tolerable since the crossovers are spaced approximately 3/4 of a wavelength apart and are also padded by the coupler between each crossover. The final input VSWR measured on the entire circuit was less than 1.16 over the 1.2 to 1.4 GHz band (Section 3).

5.6 PRINTED CIRCUIT DIPOLE

The dipole, figure 5-8, is a design developed for the Sperry AN/TPS-59 and ALR antenna. The measured VSWR of a single dipole over a ground plane was less than 1.1 at 1.3 GHz rising to 1.45 at the band edges. It is felt that this dipole will be adequate to demonstrate the performance of a single line source, and is included in the layout. Attempting to improve the VSWR at this time would not be advantageous since the dipole match is highly dependent on the spacing of the elements in an array environment. Since only a line source will be built at this time, fine tuning of the dipole VSWR will not be possible.

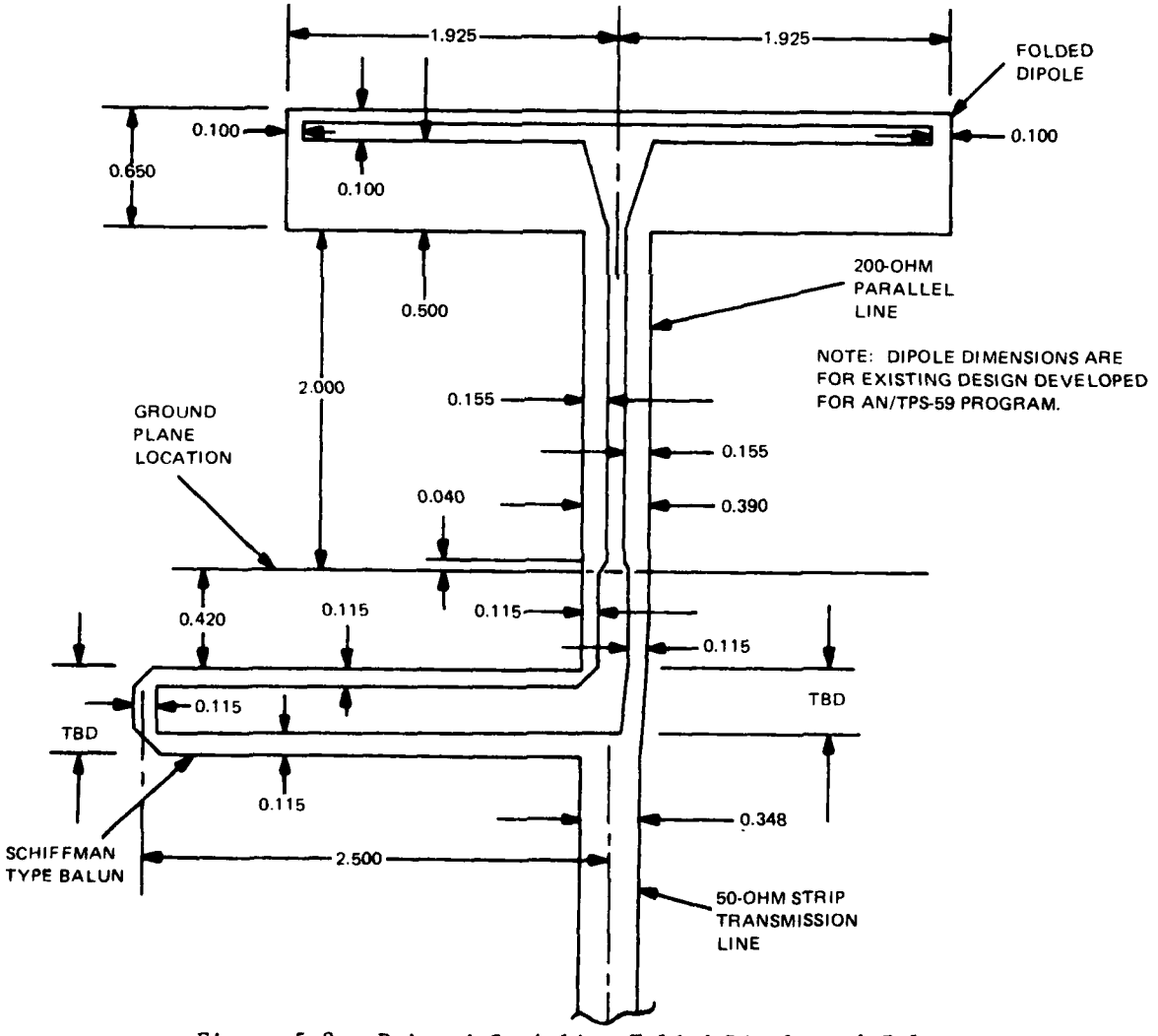

Figure 5-8. Printed Stripline Folded Dipole and Balun

Section 6

CONCLUSIONS AND RECOMMENDATIONS

The results of this program confirmed that large (12-foot) stripline dual beam column networks can be fabricated in an economical manner. The network simultaneously forms a lower pencil beam and upper csc^2 beam with less than 15 dB sidelobes, and has low insertion loss as required for an unattended radar.

The network can be built for a projected cost of $300 as a press-laminated assembly, with a weight of less than nine pounds. Additional mechanical support structures, weighing approximately 30 pounds per board, are required when the networks are assembled into an array. This is required to resist wind loads on the array face.

Utilizing these networks, along with solid state RF power amplifiers, a very power efficient and low cost unattended radar system could be built to operate in an arctic environment.

During this program one breadboard stripline dual beam network was built. It is recommended that the program be extended to build one entire array face, including the azimuth distribution networks, the 5-bit diode phase shifters and drivers, the dual beam elevation networks, and the protective radome and supporting structure.

In building the array face, the mass production manufacturing techniques would be refined, and the structural integrity of the lightweight design would be demonstrated. Also, the electrical performance of the entire phase array system would be measured by taking far-field patterns as the beams are scanned by the diode phase shifters.

MISSION
of
Rome Air Development Center

RADC plans and executes research, development, test and selected acquisition programs in support of Command, Control Communications and Intelligence (C^3I) activities. Technical and engineering support within areas of technical competence is provided to ESD Program Offices (POs) and other ESD elements. The principal technical mission areas are communications, electromagnetic guidance and control, surveillance of ground and aerospace objects, intelligence data collection and handling, information system technology, ionospheric propagation, solid state sciences, microwave physics and electronic reliability, maintainability and compatibility.

Printed by
United States Air Force
Hanscom AFB, Mass. 01731